**Assessing distinct patterns of cognitive aging using tissue-specific brain age prediction based on diffusion tensor imaging and brain morphometry**

Geneviève Richard[a,b,c,*], Knut Kolskår[a,b,c], Anne-Marthe Sanders[a,b,c] , Tobias Kaufmann[a], Anders Petersen[d], Nhat Trung Doan[a], Jennifer Monereo Sánchez[a], Dag Alnæs[a], Kristine M. Ulrichsen[a,b,c], Erlend S. Dørum[a,b,c], Ole A. Andreassen[a], Jan Egil Nordvik[c], Lars T. Westlye[a,b,*]

[a] NORMENT, KG Jebsen Centre for Psychosis Research, Division of Mental Health and Addiction, Oslo University Hospital & Institute of Clinical Medicine, University of Oslo, Norway

[b] Department of Psychology, University of Oslo, Norway

[c] Sunnaas Rehabilitation Hospital HT, Nesodden, Norway

[d] Center for Visual Cognition, Department of Psychology, University of Copenhagen, Copenhagen, Denmark

**\*Corresponding authors:**

Geneviève Richard & Lars T. Westlye

Email: genevieve.richard@medisin.uio.no, l.t.westlye@psykologi.uio.no

Postal address: Oslo University Hospital, P.O.Box 4956 Nydalen, 0424 OSLO, Norway

Telephone: +47 23 02 73 50, Fax: +47 23 02 73 33

**Short title:**

Tissue-specific brain age prediction

**Key words:**

Brain age, machine learning, white matter, gray matter, DTI, T1

**Disclosures:**

The authors declare no competing financial interests.

1 **Abstract**

2 Multimodal imaging enables sensitive measures of the architecture and integrity of the human

3 brain, but the high-dimensional nature of advanced brain imaging features poses inherent

4 challenges for the analyses and interpretations. Multivariate age prediction reduces the

5 dimensionality to one biologically informative summary measure with potential for assessing

6 deviations from normal lifespan trajectories. A number of studies documented remarkably

7 accurate age prediction, but the differential age trajectories and the cognitive sensitivity of

8 distinct brain tissue classes have to a lesser extent been characterized.

9 Exploring differential brain age models driven by tissue-specific classifiers provides a

10 hitherto unexplored opportunity to disentangle independent sources of heterogeneity in brain

11 biology. We trained machine-learning models to estimate brain age using various

12 combinations of FreeSurfer based morphometry and diffusion tensor imaging based indices of

13 white matter microstructure in 612 healthy controls aged 18-87 years. To compare the tissue-

14 specific brain ages and their cognitive sensitivity we applied each of the 11 models in an

15 independent and cognitively well-characterized sample (n=265, 20-88 years). Correlations

16 between true and estimated age in our test sample were highest for the most comprehensive

17 brain morphometry (r=0.83, CI:0.78-0.86) and white matter microstructure (r=0.79, CI:0.74-

18 0.83) models, confirming sensitivity and generalizability. The deviance from the

19 chronological age were sensitive to performance on several cognitive tests for various models,

20 including spatial Stroop and symbol coding, indicating poorer performance in individuals

21 with an over-estimated age. Tissue-specific brain age models provide sensitive measures of

22 brain integrity, with implications for the study of a range of brain disorders.

23

24

25

26

27

28

29

30

31

32

33

## Introduction

Increasing age is a major risk factor for cognitive decline and neurodegeneration, and deviating lifespan trajectories in brain structure and function is a sensitive marker in several common neurological and mental disorders (Cole & Franke 2017). The maturing and aging brain is highly heterogeneous in term of individual trajectories and in term of brain regions and mechanisms involved (Fjell et al. 2013; Westlye et al. 2010b). Understanding the individual determinants and heterogeneity of the developing and aging brain is imperative for identifying persons at risk for various brain disorders, and for developing and applying effective and targeted treatments.

Exploring different modalities acquired by magnetic resonance imaging (MRI) provide a powerful tool to investigate age-related differences in both gray- and white- matter tissue classes across brain regions. However, the richness and complexity of the information provided by advanced imaging pipelines challenges its interpretation. Together, the multifactorial age-related variability and the richness of imaging measures have motivated the development of biologically informative summary measures based on brain imaging data. Using machine-learning to estimate the biological age of the brain based on neuroimaging data is one such approach (Cole & Franke 2017; Cole et al. 2018; Kaufmann et al. 2018). Deviation from the normative trajectory is a highly relevant biomarker for the integrity of the brain in healthy and clinical populations (Marquand et al. 2016; Wolfers et al. in press). Brain age gap is a heritable trait showing regionally specific genetic overlaps with major brain disorders, including schizophrenia and multiple sclerosis (Kaufmann et al. 2018), and accumulating evidence supports increased brain age in several clinical groups, including patients with schizophrenia (Kaufmann et al. 2018; Schnack et al. 2016), Alzheimer's disease (Amoroso et al. 2017; Kaufmann et al. 2018), HIV (Cole et al. 2017b; Kuhn et al. 2018) multiple sclerosis (Kaufmann et al. 2018) and cardiovascular risk factors (Franke et al. 2013; Habes et al. 2016). Indeed, while individuals with brains estimated as younger than their chronological age have been shown to be more physically active (Steffener et al. 2016), augmented brain age has been associated with poor health (Ronan et al. 2016), poor cognitive performance (Liem et al. 2017), early neurodegenerative diseases (Gaser et al. 2013), and increased mortality (Cole et al. 2017a). Less is known about the regional heterogeneity, i.e. to which degree different brain regions, systems or compartments show differential aging patterns and sensitivity to cognitive performance. Brain gray and white matter compartments, which can be assessed and quantified using T1-weighted imaging and diffusion tensor

67    imaging (DTI), respectively, comprise distinct tissue classes with largely differential

68    biological and environmental modifiers and age trajectories (Bennett et al. 2010; Cao et al.

69    2017; Fjell et al. 2013; Salat et al. 2005; Storsve et al. 2014; Westlye et al. 2010a; Westlye et

70    al. 2010b). Therefore, allowing for differential brain age models for these distinct classes

71    provides an opportunity to disentangle independent sources of heterogeneity in brain aging.

72         Thus, to identify common and unique aging patterns with potentially differential

73    sensitivity to cognitive function, we aimed to test the complementary value of tissue-specific

74    prediction by comparing brain age estimated using different combinations of FreeSurfer based

75    morphometric measures (regional cortical thickness, surface area and volume) and white

76    matter microstructure features (DTI based fractional anisotropy and mean, radial and axial

77    diffusivity) across the brain. Based on previous studies on brain aging, we expected high

78    accuracy and generalizability of the age prediction models (Cole & Franke 2017). Since tissue

79    specific brain age models capture biologically distinct information, we anticipated that the

80    different FreeSurfer based brain morphometry and white matter microstructure models would

81    only partly reflect common variance, and therefore provide complementary information with

82    differential sensitivity to cognitive performance. Given that brain age predictions might be

83    sensitive to the overall integrity of the brain (Liem et al. 2017), we anticipated that individuals

84    with an over-estimated brain age would show lower cognitive performance, in particular

85    among the elderly, and that the tissue-specific brain age models would show partly

86    differential cognitive sensitivity.

87         To ensure generalizability, we trained the models in a large publicly available training

88    set (n=612, 18-87 years) and validated their performance using 10-fold cross-validation

89    before applying to an independent and well characterized test set (n=265, 20-88 years). We

90    assessed the cognitive sensitivity using linear and non-linear models with performance on a

91    range of paper-and-pencil and computerized tests comprising different large-scale cognitive

92    domains (processing speed, executive functioning, working memory, attention, and general

93    intellectual abilities) and cognitive scores based on computational models as dependent

94    variables and age, sex and brain age gap (BAG, estimated brain age minus chronological age)

95    as independent variables. For transparency, we report results both at an uncorrected level and

96    corrected using false discovery rate (FDR) and Bonferroni methods to control the error rate.

97

98

99

100 **Materials and methods**

101 Table 1 summarizes key demographics. We included data from healthy volunteers from two

102 independent cohorts: (1) the Cambridge Centre for Ageing and Neuroscience (Cam-CAN)

103 sample (http://www.mrc-cbu.cam.ac.uk/datasets/camcan/; (Shafto et al. 2014; Taylor et al.

104 2017)) and (2) StrokeMRI, which is an ongoing study on the determinants of stroke recovery,

105 brain health and successful aging (Dorum et al. 2016; Dorum et al. 2017). Figure 1 shows the

106 age distribution for each sample.

107 Volunteers were recruited to Cam-CAN through a large-scale collaborative research

108 project funded by the Biotechnology and Biological Sciences Research Council (BBSRC,

109 grant number BB/H008217/1), the UK Medical Research Council and University of

110 Cambridge. For more information, see www.cam-can.org. Among the 650 datasets made

111 available, 17 were excluded based on missing or poor quality DTI data and 21 due to poor

112 T1-weighted data quality. Data from the remaining 612 individuals (age 18-87, mean = 54.41,

113 SD = 18.26, 314 females) were included.

114 Healthy individuals were recruited to StrokeMRI through advertisement in

115 newspapers, social media and word-of-mouth. All participants completed a comprehensive

116 cognitive assessment, multimodal MRI and blood sampling for clinical biochemical analysis,

117 various biomarkers and genotyping. MRI and cognitive assessments were performed on two

118 subsequent days. Exclusion criteria included history of stroke, dementia, or other neurologic

119 and psychiatric diseases, alcohol- and substance abuse, medications significantly affecting the

120 nervous system and counter indications for MRI. In addition, individuals scoring lower than

121 25 on the Montreal Cognitive Assessment (MoCA; Nasreddine et al. 2005) were assessed for

122 inclusion based on their age, level of education and performance on other cognitive tests. No

123 participants were excluded based on a single low score. A neuroradiologist reviewed all scans

124 and 14 participants with clinically significant abnormalities were excluded. Additional

125 exclusion criteria included missing or incomplete MRI or cognitive data (n=2), or poor

126 quality images (n=20). The remaining 265 participants (age 20-88, mean = 56.95, SD = 14.84,

127 168 females) were included in further analyses. The study was approved by the Regional

128 Committee for Medical and Health Research Ethics (South-East Norway), and conducted in

129 accordance with the Helsinki declaration. All subjects signed an informed consent prior to

130 participating and received a compensation for their participation.
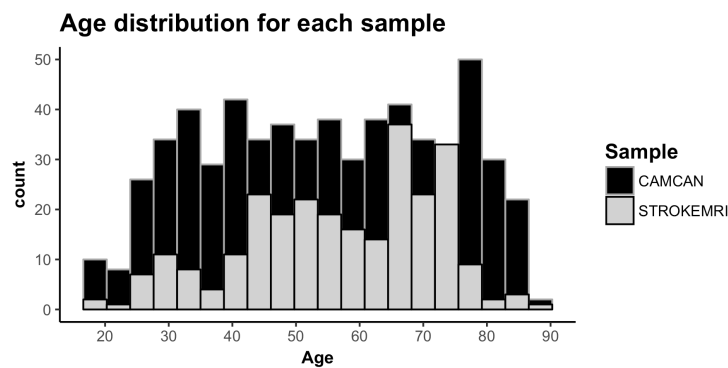
131

132

133



**Fig. 1** Histogram of the age distribution for each sample.

141

142 *Cognitive assessment in StrokeMRI*

143 Cognitive performance was assessed with a set of neuropsychological and computerized tests

144 assumed to be sensitive to cognitive aging, including the MoCA, the vocabulary and matrix

145 subtests of the Wechsler Abbreviated Scale of Intelligence (WASI; Wechsler 1999), the

146 California Verbal Learning Test (CVLT-II; Delis et al. 2000), and the Delis-Kaplan Executive

147 Function System (D-KEFS) color word interference test (Stroop; Delis et al. 2001). We

148 included several computerized tests from the Cognitive Assessment at Bedside for iPAD

149 (CABPad; Willer et al. 2016), including motor speed, verbal fluency (phonological and

150 semantic), working memory, spatial Stroop (executive control of attention), spatial attention

151 span, and symbol digit coding tests. In addition, in order to assess the specificity of cognitive

152 associations using computation modeling, we included three mathematically independent

153 parameters based on the Theory of Visual Attention (TVA; Bundesen 1990; Bundesen &

154 Habekost 2008), including short-term memory storage ($K$), processing speed ($C$), perceptual

155 threshold ($t_0$). These parameters based on computational modeling of response patterns have

156 been shown to be sensitive to age, brain structure and function in healthy individuals

157 (Espeseth et al. 2014; Wiegand et al. 2018) and a range of brain disorders (Habekost 2015;

158 Habekost & Starrfelt 2009). Here, we used a TVA-based modeling of a whole report

159 (Sperling 1960), in which six letters were briefly presented for different exposure durations

160 and the participant's task was to accurately report as many letters as possible. Task error rate

161 was also assessed (i.e. number of incorrect letters out of reported letters).

162

163 *MRI acquisition*

164 Cam-CAN participants were scanned on a 3T Siemens TIM Trio scanner with a 32-channel

165 head-coil at Medical Research Council (UK) Cognition and Brain Sciences Unit (MRC-

166    CBSU) in Cambridge, UK. DTI data was acquired using a twice-refocused spin echo

167    sequence with the following parameters a repetition time (TR) of 9100 ms, echo time (TE) of

168    104 ms, field of view (FOV) of 192 x 192 mm, voxel size: 2 mm$^3$, 66 axial slices using 30

169    directions with b= 1000 s/mm$^2$, 30 directions with b= 2000 s/mm$^2$, and 3 b=0 images (Shafto

170    et al. 2014). Only the b=[0,1000] were used in the current analysis. High-resolution 3D T1-

171    weighted data was acquired using a magnetization prepared rapid gradient echo (MPRAGE)

172    sequence with the following parameters: TR: 2250 ms, TE: 2.99 ms, inversion time (TI): 900

173    ms, flip angle (FA): 9°, FOV of 256 x 240 x 192mm; voxel size =1 mm$^3$ isotropic, GRAPPA

174    acceleration factor of 2, scan time 4:32 minutes (Shafto et al. 2014).

175    StrokeMRI participants were scanned on a 3T GE 750 Discovery MRI scanner with a

176    32-channel head coil at Oslo University Hospital. Paddings were used to reduce head motion.

177    DTI data were acquired using an echo planar imaging (EPI) sequence with the following

178    parameters: TR/TE/flip angle: 8150 ms/83.1 ms/90°, FOV: 256 x 256 mm, slice thickness: 2

179    mm, in-plane resolution: 2 mm, 60 directions (b=1000 s/mm$^2$) and 5 b=0 volumes, scan time:

180    8:58 min. In addition, 7 b=0 volumes with reversed phase-encoding direction were acquired.

181    High-resolution T1-weighted data was acquired using a 3D IR-prepared FSPGR (BRAVO)

182    with the following parameters: repetition time: 8.16 ms, echo time: 3.18 ms, flip angle: 12º,

183    voxel size: $1 \times 1 \times 1$ mm, field of view: 256 x 256 mm, 188 sagittal slices, scan time: 4:43

184    minutes.

185

186    *DTI processing and analysis*

187    Diffusion MRI data from both samples were processed locally using the Oxford Center for

188    Functional Magnetic Resonance Imaging of the Brain (FMRIB) Software Library (FSL)

189    (http://www.fmrib.ox.ac.uk/fsl). To correct for geometrical distortions, motion and eddy

190    currents, data were preprocessed using topup (https://fsl.fmrib.ox.ac.uk/fsl/fslwiki/topup) and

191    eddy (https://fsl.fmrib.ox.ac.uk/fsl/fslwiki/eddy) respectively (Andersson et al. 2003; Smith et

192    al. 2004). Topup uses information from the reversed phase-encoded image, resulting in pairs

193    of images (blip-up, blip-down) with distortions going in opposite directions. From these

194    image pairs the susceptibility-induced off-resonance field was estimated and the two images

195    were combined into a single corrected one (Andersson et al. 2003; Smith et al. 2004). This

196    step was performed on StrokeMRI data only. Eddy detects and replaces slices affected by

197    signal loss due to bulk motion during diffusion encoding, which is performed within an

198    integrated framework along with correction for susceptibility induced distortions, eddy

199   currents and motion (Andersson & Sotiropoulos 2016). Although these processing steps have

200   been shown to strongly increase the temporal signal-to-noise ratio (tSNR) (Doan et al. 2017),

201   we performed additional visual inspection to identify and remove poor quality data.

202         Fractional anisotropy (FA), eigenvector, and eigenvalue maps were calculated using

203   dtifit in FSL. Mean diffusivity (MD) was defined as the mean of all three eigenvalues, radial

204   diffusivity (RD) as the mean of the second and third eigenvalue, and axial diffusivity (AD) as

205   the principal eigenvalue.

206         Voxelwise analysis of FA, MD, AD and RD were carried out using Tract-Based

207   Spatial Statistics (TBSS; Smith et al. 2006), part of FSL (Smith et al. 2004). First, all subjects'

208   FA data were aligned to a common space using the nonlinear registration tool FNIRT

209   (Andersson et al. 2007a; Andersson et al. 2007b). Next, the mean FA image was created and

210   thinned to create a mean FA skeleton, which represents the centers of all tracts common to all

211   participants. Each subject's aligned FA data was then projected onto this skeleton and the

212   resulting data fed into voxelwise cross-subject statistics. The same warping and

213   skeletonization was repeated for MD, AD and RD. We thresholded and binarized the mean

214   FA skeleton at FA>0.2. For each individual, we calculated the mean skeleton FA, MD, AD

215   and RD, as well as mean values within 23 regions of interest (ROIs) based on two

216   probabilistic white matter atlases provided with FSL, i.e. the CBM-DTI-81 white-matter

217   labels atlas and the JHU white-matter tractography atlas (Hua et al. 2008; Mori et al. 2005;

218   Wakana et al. 2007), yielding a total of 96 DTI features per individual.

219

220   *T1 processing*

221   T1-weighted images were processed using FreeSurfer 5.3 (http://surfer.nmr.mgh.harvard.edu;

222   (Dale et al. 1999)) including brain extraction, intensity normalization, automated tissue

223   segmentation, generation of white and pial surfaces (Dale et al. 1999). All reconstructions

224   were visually assessed and corrected as appropriate. Cortical parcellation was performed

225   using the Desikan–Killiany atlas (Desikan et al. 2006; Fischl et al. 2004) and subcortical

226   segmentation was performed based on a probabilistic atlas (Fischl et al. 2002). In addition to

227   global features (intracranial volume, total surface area, whole-cortex mean thickness), mean

228   thickness, total surface area, and volume for each cortical ROI, as well as the volume of

229   subcortical structures were computed yielding a set of 251 FreeSurfer based features.

230

231

232    *Age prediction*

233    Eleven different models were trained to estimate age based on the feature sets described

234    above (one based on FreeSurfer T1 features, one based on WM DTI features, one including

235    all T1 and DTI features, in addition to eight models based on a smaller subset of features,

236    including models based on FA, MD, AD, RD, sub-cortical volume, volume, area and

237    thickness to further explore the modality specificity of the estimations).

238         Due to the systematic differences in the brain features across scanners as well as non-

239    linear effects of age, we fit a generalized additive model (GAM; Hastie 2017) for each feature

240    and regressed out the effects of scanning site and age$^2$, accounting all models for age and sex.

241    In addition, we regressed out the estimated total intracranial volume from the area and volume

242    features. Next, for each model, we created a training data matrix by concatenating all the

243    features for all participants in the training sample (Cam-CAN), which were used as input to

244    estimate age. We used the *xgboost* framework in R (http://xgboost.readthedocs.io/en/latest/R-

245    package/xgboostPresentation.html), an efficient and scalable implementation of gradient

246    boosting machine learning techniques, to build the prediction models. The following

247    parameters were used: learning rate (eta) = 0.1, nround = 5000, gamma = 1, max_depth = 6,

248    subsample=0.5. To estimate the performance of our models, we used a 10-fold cross-

249    validation procedure within the training sample and repeated the cross-validation step 1000

250    times to provide a robust estimate of model predictive accuracy. Next, we tested the

251    performance of our trained models by predicting age in unseen healthy subjects in the test

252    sample (StrokeMRI).

253         For each feature set, we calculated the correlation between the predicted and the

254    chronological age as a measure of the model performance, in addition to the mean absolute

255    error (MAE, in years). For each individual, we calculated the discrepancy between the

256    estimated and the chronological age, i.e. the BAG, for each model. The MAE was calculated

257    from the BAG for each model. Since we were interested in the effect of BAG independently

258    of age, the effect of age was regressed out for each BAG using linear models.

259

260    *Statistical analysis*

261    Statistical analysis was performed using R (http://www.r-project.org). For cognitive data, we

262    used *outlierTest* from the car package (Fox & Weisberg 2011) to identify the most extreme

263    observations based on a linear model, including age and sex. Twenty-five observations were

264    identified as outliers and treated as missing values based on a Bonferroni corrected p < 0.05.

265    To visualize the associations between the cognitive tests and to form cognitive domain scores

266    based on the correlation patterns, we performed hierarchical clustering using the default

267    setting of the heatmap.2 package in gplots (Warnes et al. 2016), which uses hclust (Müllner

268    2013) to form clusters based on the complete linkage method. Briefly, this is a step-wise

269    clustering process that merges the two nearest clusters until only one single cluster remains,

270    maximizing distance between individuals components between two clusters.

271        For each cognitive measure and summary score based on the clusters formed form the

272    clustering step above, we used linear models to test for the effect of age and sex. Since

273    cognitive performance may show non-linear associations with age, we performed an

274    additional analysis including both age and $age^2$ in the models. Then, for each test showing a

275    significant association with age, we tested whether adding BAG to the models lead to an

276    improved model fit. More specifically, we tested for differential associations with cognitive

277    function by comparing the parameter estimates for the different BAG models using Fisher z-

278    transformation. To test the assumption that increased BAG is more relevant for cognitive

279    function among the elderly, we tested for age by BAG interactions on cognitive performance.

280    For transparency, we report both uncorrected p-values and p-values adjusted using FDR

281    (Benjamini & Hochberg 1995; Wright 1992) and Bonferroni correction using a factor of 495

282    (11 brain gaps and 45 cognitive features).

283

284    **Results**

285    *Brain age prediction*

286    10-fold cross-validation on the training sample revealed high correlations between

287    chronological and predicted age for the DTI based white matter microstructure (r=0.87) and

288    FreeSurfer based morphometric (r=0.88) models. Likewise, the correlations for FA (r=.76),

289    MD (r=.80), AD (r=.83), RD (r=78), sub-volume (r=.84), volume (r=.80), area (r=.70) and

290    thickness (r=.79) based models also confirmed reasonable model performance.

291        Most models accurately predicted age in the independent test set. Figure 2A shows a

292    correlation matrix for the 11 BAGs. Figure 2B shows the correlations between the

293    chronological age and the predicted age in the test sample for each model with their

294    confidence intervals, ranging from (r=.86, CI:.82-.89, MAE= 6.14) for the combined model to

295    r=.58 (CI:.49-.65, MAE=10.24) for the model based on area. Figure 2 (D to F) show the

296    estimated age from the three models that performed best among the 11 feature sets, i.e. the

297 combined DTI and T1 feature models (r=.86, CI:.82-.89, MAE= 6.14), the 251 FS T1 features

298 (r=.83, CI:.78-.86, MAE= 6.76), and the 96 WM DTI features (r=.79, CI:.74-.83, MAE=7.28).

299



**Fig. 2** Comparison between the 11 BAG models. (a) Heatmap of the correlation between different BAGs. (b) Correlations between the chronological age and the predicted age in the test sample for each model with their confidence intervals. (c) Mean and standard error of the 45 p-values ($-\log_{10}(p)$) for the cognitive scores and composite scores for each row (i.e. BAGs), with a higher mean representing a stronger global association across tests. (d) Correlation between the chronological age of each subjects and the combined age, (e) the brain morphometry age, and (f) the white matter microstructure age.

*Cognitive assessments and associations with BAGs*

Table 1 summarizes descriptive statistics and associations with age and sex for each of the 49 cognitive scores, derived features and domain scores. Linear models revealed 45 significant associations with age after correcting for multiple comparisons, with the strongest effect sizes for the symbol coding test, motor speed, spatial Stroop and spatial attention span. Since non-linear models revealed significant associations with age$^2$ only with the color word Stroop 3 (inhibition) and its derived scores (See supplementary Table S1), the main models presented here are linear in order to keep the model to its simplest form. Figure 3 shows a correlation matrix across all normalized cognitive scores with the variables sorted according to the

319   hierarchical clustering. Several variables were highly correlated, and the clustering solution

320   generally suggested seven broad cognitive domains including (Cluster 1) memory and

321   learning (CVLT, attention span, MoCA), (Cluster 2) visual processing speed (TVA

322   processing speed and perceptual threshold), (Cluster 3) verbal skills (phonological and

323   semantic flow), (Cluster 4) attentional control and speed (spatial Stroop), (Cluster 5)

324   executive control and speed (color-word Stroop), (Cluster 6) reasoning and psychomotor

325   speed (matrix, symbol coding and motor speed, short-term memory storage (TVA-parameter

326   *K*)), and (Cluster 7) working memory.

327
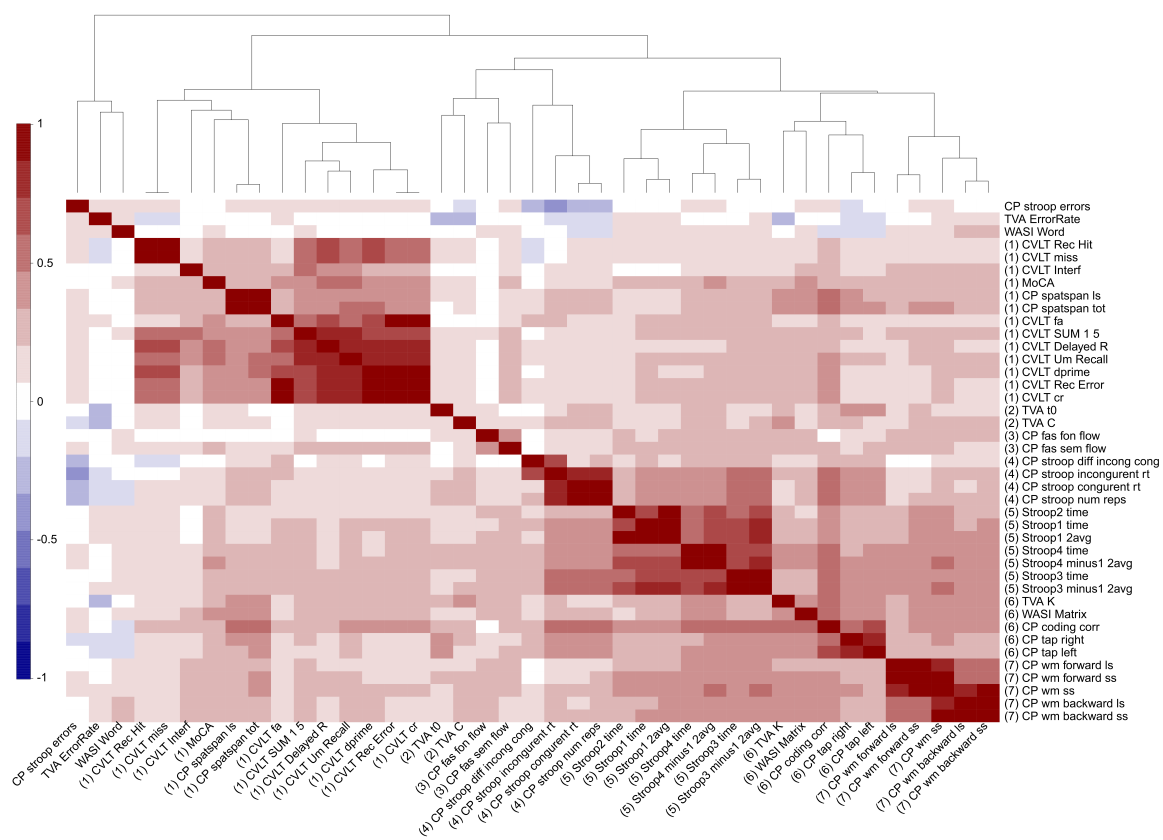


328

**Fig. 3** Hierarchical clustering of the cognitive features. Each cognitive score was normalized and when required the scores were multiplied by -1 to ensure that positive scores represent good performance. The higher panel shows the dendrogram resulting from the hierarchical clustering of the scores in 7 cognitive domains.

333   Table 2 shows summary statistics for the associations between cognitive performance and

334   BAG using linear models, including age and sex as covariates. Figure 4 shows a heatmap of

335   the association between cognitive scores and brain age gaps for which the significant

336   associations have been marked with an asterisk. Supplementary Table S1 and Fig. S1 shows

337      the summary statistics and the heatmap of the associations between cognitive performance

338      and BAG using non-linear models. Figure 2C shows the mean and standard error of the 45 p-

339      values (-$\log_{10}(p)$) for the cognitive scores and composite scores for each row (i.e. BAGs),

340      with a higher mean representing a stronger cumulative association across tests.

341         Figure 5 shows a scatter plot of the 2 strongest associations, which were found

342      between the most comprehensive model (all features combined) and spatial Stroop congruent

343      trials and number of responses, respectively, indicating poorer performance with higher BAG.

344      Fisher z-transformation revealed no statistically significant differences in the cognitive

345      associations between linear models using tissue-specific BAG. No significant interactions

346      were found between BAG and age on cognitive performance.

347



**Associations between cognitive tests and BAG**
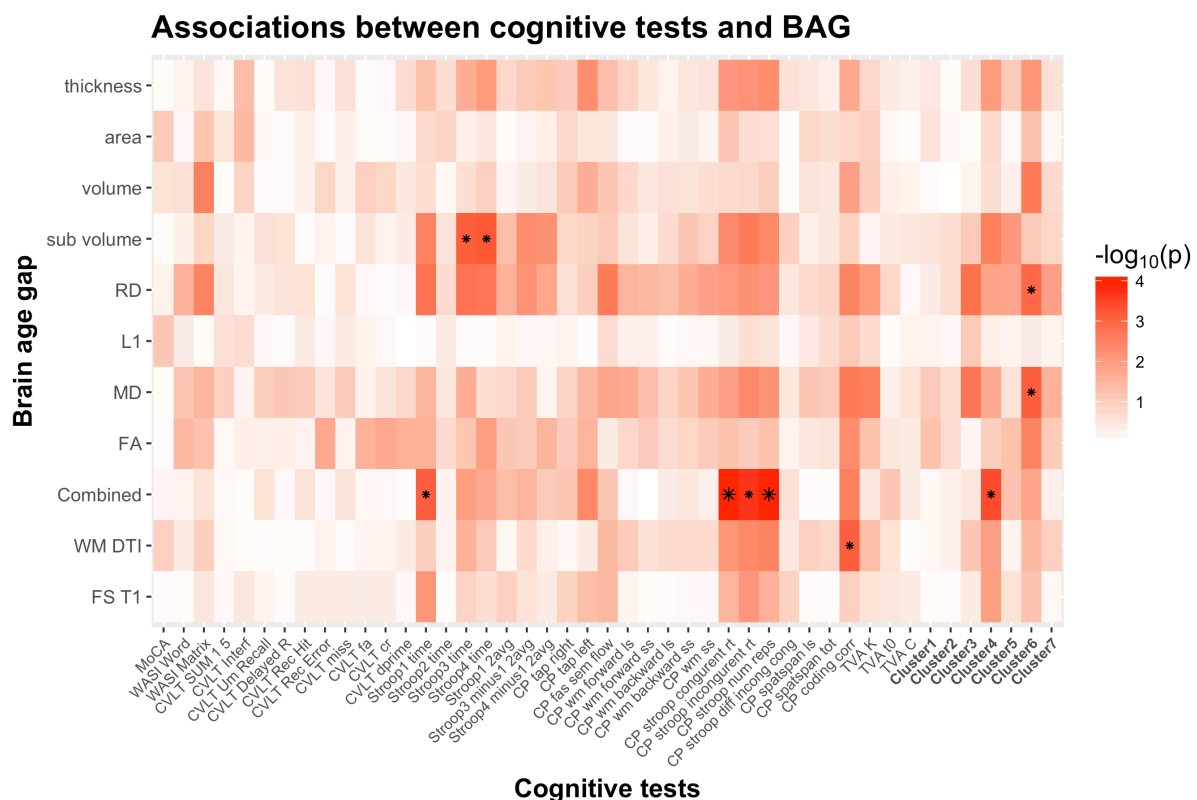
348

349      **Fig. 4** Heatmap of the association between cognitive scores and brain age gaps. The color

350      scale depicts the minus log of the p-values (-$\log_{10}(p)$) for each association. The association

351      marked with a small star represents significant associations after FDR correction, and the one

352      marked with a big star shows significant associations after Bonferroni correction.

353

354
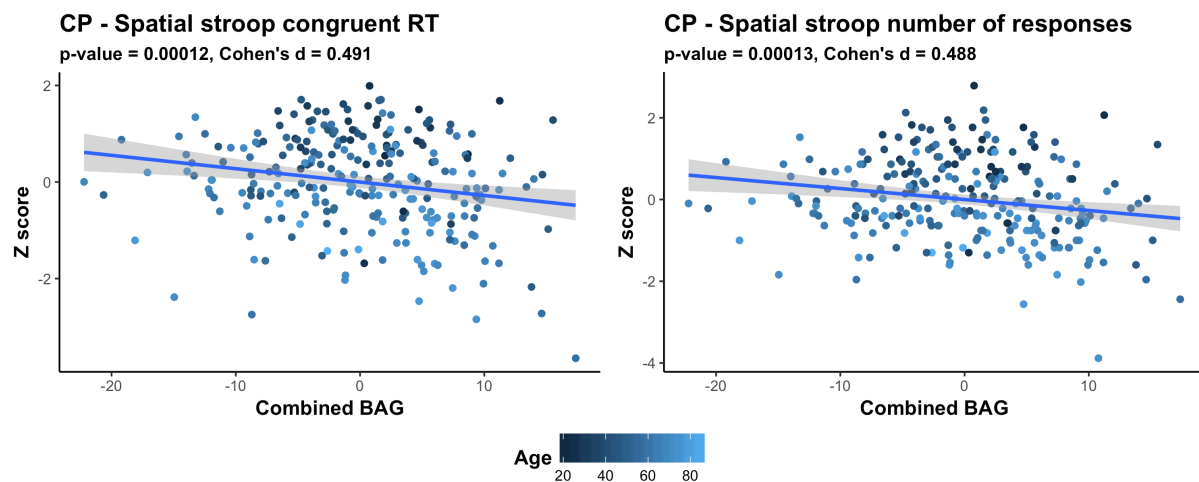
**Fig. 5** Scatter plots of the 2 strongest associations between cognitive measures and BAG. The color gradient represents the age where lighter color is assigned to older individuals, and darker color to younger individuals. All associations indicate worse performance with higher brain age gap.

**Discussion**

Brain aging is highly heterogeneous, and expanding our understanding of the biological determinants of human aging is imperative for reducing the burden of age-related cognitive decline and neurodegenerative disorders. An estimate of an individual's deviation from the expected lifespan trajectory in brain structure and function may provide a sensitive measure of individual brain integrity and health, both in presumably healthy individuals and in patients suffering from various brain disorders.

The biological heterogeneity of the brain strongly suggests that the concept of a single brain age is too simple, and that tissue-specific brain age models may provide increased sensitivity and specificity in relation to cognitive and mental functions. In line with this view, our main findings demonstrate that different combinations of FreeSurfer based brain morphometry and DTI based white matter microstructural indices can be used to accurately predict the age of individuals, but that the shared variance from the different models suggest that they reflect partly non-overlapping processes of brain aging. Further, the results revealed partly differential sensitivity to cognitive performance; with the strongest cumulative associations across cognitive tests for brain age gaps estimated using RD. Even though our data provide no strong evidence of independent associations with cognitive performance in the current sample of healthy individuals, tissue specific age prediction models might better

379    inform us about the individual determinants and heterogeneity of the aging brain compared to

380    models collapsing several brain compartments by potentially capturing distinct measures of

381    brain aging.

382

383    *Brain age prediction*

384    For the age prediction models, our results demonstrated that the 11 different combinations of

385    FreeSurfer based morphometric measures (regional cortical thickness, surface area and

386    volume) and white matter microstructure features (diffusion tensor imaging (DTI) based

387    fractional anisotropy and mean, radial and axial diffusivity) across the brain age models

388    accurately predicted the age of an individual with a mean absolute error between 6.14 and

389    10.23 years. Brain morphometry and white matter microstructure models had a MAE of 6.76

390    and 7.28 respectively, which correspond with previous publications (Cole et al. 2016; Han et

391    al. 2014; Valizadeh et al. 2017). In general, combining features and modalities increased the

392    performance, and the highest performing model included a combination of both brain

393    morphometry and white matter microstructure (mean absolute error of 6.14 years). Moreover,

394    the correlations between the different brain age gaps suggested a relatively low level of shared

395    variance (mean correlation = 0.51, SD=0.13). Together these findings support the notion that

396    tissue specific brain age models capture biologically distinct information. This is in line with

397    the characteristic lifespan patterns of global linear decreases in gray matter volume and the

398    nonlinear trajectories of total white matter volume and DTI based metrics of white matter

399    microstructure (Cox et al. 2016; Fjell et al. 2013; Ge et al. 2002; Liu et al. 2017; Raz et al.

400    2010; Westlye et al. 2010b), highlighting that the different compartments carry unique

401    biological information and that combining different modalities lead to a better estimation the

402    age of individuals (Cherubini et al. 2016; Liem et al. 2017; Madan & Kensinger 2018).

403

404    *Cognitive associations*

405    We performed a comprehensive cognitive assessment of the test sample, confirming previous

406    evidence of substantial age-related differences in cognitive performance across a range of

407    tests and domains. Hierarchical clustering of the cognitive features indicated a characteristic

408    pattern of covariance, largely reflecting broad cognitive domains, including memory and

409    learning, visual processing speed, verbal skills, attentional and executive control, reasoning

410    and psychomotor speed, and working memory. Ninety percent of the included cognitive

411    features showed age-differences, with the largest effect sizes observed for speed-based

412  measures, such as symbol coding test, which measures mental and visuo-motor speed (Willer

413  et al. 2016). This is in line with the well-established literature on age-related decline in

414  information processing speed in healthy aging (Bennett et al. 2010; Craik & Salthouse 2008;

415  Harada et al. 2013). Importantly, not only tasks measuring reaction time, but also various

416  TVA measures based on computational modeling, such as short-term memory storage ($K$),

417  processing speed ($C$), and perceptual threshold ($t_0$) showed strong associations with age, in

418  line with previous studies (Espeseth et al. 2014; Habekost 2015; Habekost et al. 2013;

419  McAvinue et al. 2012; Wiegand et al. 2018).

420       Based on the assumption that brain age captures variance related to the integrity of the

421  brain, we anticipated that individuals with an over-estimated age would show lower cognitive

422  performance, and that the tissue-specific brain age models would show partly differential

423  sensitivity. To test these hypotheses, we used linear models to explore the associations

424  between cognitive performance and BAG, with age and sex as covariates, and directly

425  compared the parameter estimates from the different brain age models. We found a significant

426  association between performance on several tests and BAG beyond the age associations,

427  indicating lower performance in individuals with higher BAG. Briefly, one significant

428  association was found for WM DTI, five for combined BAG, two for the sub-volume, one for

429  the RD and one for the MD BAG. The strongest associations were found with the spatial

430  Stroop congruent trials, and number of responses. These findings support that the deviance

431  between the estimated age and the chronological age captures relevant biological information

432  regarding the cognitive performance of an individual. Whereas we found no significantly

433  different associations between brain age models, the association with symbol digit coding test

434  was only seen for WM DTI BAG, while associations with Stroop 3 and 4 were observed only

435  for sub-volume BAG, suggesting some specificity that should be investigated in future studies

436  including larger samples and a broader spectrum of mental health, cognitive and brain

437  phenotypes, both across healthy and clinical samples. We speculate that the contributions of

438  the different modalities in predicting age and the associations with both cognitive

439  performance, but also age-related illnesses vary across the age-span, as it does during

440  maturational age (Brown et al. 2012). Thus, future studies might benefit from investigating

441  modality specific brain-age estimation using specific age range.

442

443

444

445 *Limitations*

446 The present findings do not come without limitations. First, although reducing the

447 dimensionality of complex brain imaging data to a biologically informative brain age is a

448 powerful method to assess deviations from normal lifespan trajectories in brain health,

449 findings from this data reduction method are limited in specificity. Here, we attempted to both

450 reduce the complexity of the information while keeping some modality specificity measured

451 by different MRI parameters. Finding a balance between specificity and precision represents

452 an interesting challenge for future studies. Moreover, causality and individual level

453 trajectories cannot be established based on cross-sectional data. Therefore, future longitudinal

454 studies are needed to inform us about the relevance of the differential trajectories of the

455 tissue-specific brain age prediction with implications for the study of a range of brain

456 disorders. Next, although the age distribution of the test sample is irrelevant to the individual

457 prediction accuracy, the relative overrepresentation of older individuals in the test sample is a

458 limitation when investigating interactions between BAG and age. Thus, although the lack of

459 brain by BAG interactions on cognitive function did not support our hypothesis that increased

460 BAG is more relevant for cognitive function among the elderly, future studies including

461 individuals across a broader range of function are needed to characterize the lifespan

462 dynamics in the associations between brain and behavior. Although we covered a relatively

463 broad spectrum of structural brain features, the link between imaging based indices of brain

464 structure and brain function is elusive, and brain age models including other brain imaging

465 features, including functional measures, might provide a sensitive supplement to the current

466 models. Lastly, whereas the results showed some numerical differences in the cognitive

467 sensitivity of the different combinations of FreeSurfer based morphometry and white matter

468 microstructure models, these differences were not statistically significant, and the hypothesis

469 that tissue specific models provide increased specificity in terms of cognitive associations

470 remains to be further explored in future studies.

471     In conclusion, we have demonstrated that models based on different combinations of

472 brain morphometry and white matter microstructural indices provide partly differential

473 information about the aging brain, emphasizing the relevance of tissue-specific brain age

474 models in the study of brain and mental function in health and disease.

475

476

477

478 **Acknowledgements**

479 This study was supported by the Norwegian ExtraFoundation for Health and Rehabilitation

480 (2015/FO5146), the Research Council of Norway (249795, 248238), the South-Eastern

481 Norway Regional Health Authority (2014097, 2015044, 2015073), Sunnaas Rehabilitation

482 Hospital, and the Department of Psychology, University of Oslo, and approved by the

483 Regional Committee for Medical and Health Research Ethics (South-East). Volunteers were

484 recruited to StrokeMRI through advertisement in newspapers, social media and word-of-

485 mouth. In addition, volunteers were recruited to Cam-CAN through a large-scale

486 collaborative research project funded by the Biotechnology and Biological Sciences Research

487 Council (BBSRC, grant number BB/H008217/1), the UK Medical Research Council and

488 University of Cambridge.

489

490

491

492

493

494

495

496

497

498

499

500

501

502

503

504

505

506

507

508

509

510

## References

Amoroso N, Diacono D, Fanizzi A, La Rocca M, Monaco A, Lombardi A, Guaragnella C, Bellotti R, Tangaro S, and Alzheimer's Disease Neuroimaging I. 2017. Deep learning reveals Alzheimer's disease onset in MCI subjects: results from an international challenge. *J Neurosci Methods*. 10.1016/j.jneumeth.2017.12.011

Andersson JLR, Jenkinson M, and Smith S. 2007a. TR07BP1: Non-linear optimisation. FMRIB Analysis Group Technical Reports: FMRIB Analysis Group.

Andersson JLR, Jenkinson M, and Smith S. 2007b. TR07JA2: Non-linear registration, aka spatial normalization. FMRIB Analysis Group Technical Reports: FMRIB Analysis Group.

Andersson JLR, Skare S, and Ashburner J. 2003. How to correct susceptibility distortions in spin-echo echo-planar images: application to diffusion tensor imaging. *Neuroimage* 20:870-888. 10.1016/S1053-8119(03)00336-7

Andersson JLR, and Sotiropoulos SN. 2016. An integrated approach to correction for off-resonance effects and subject movement in diffusion MR imaging. *Neuroimage* 125:1063-1078. 10.1016/j.neuroimage.2015.10.019

Benjamini Y, and Hochberg Y. 1995. Controlling the False Discovery Rate - a Practical and Powerful Approach to Multiple Testing. *Journal of the Royal Statistical Society Series B-Methodological* 57:289-300.

Bennett IJ, Madden DJ, Vaidya CJ, Howard DV, and Howard JH, Jr. 2010. Age-related differences in multiple measures of white matter integrity: A diffusion tensor imaging study of healthy aging. *Hum Brain Mapp* 31:378-390. 10.1002/hbm.20872

Brown TT, Kuperman JM, Chung Y, Erhart M, McCabe C, Hagler DJ, Jr., Venkatraman VK, Akshoomoff N, Amaral DG, Bloss CS, Casey BJ, Chang L, Ernst TM, Frazier JA, Gruen JR, Kaufmann WE, Kenet T, Kennedy DN, Murray SS, Sowell ER, Jernigan TL, and Dale AM. 2012. Neuroanatomical assessment of biological maturity. *Curr Biol* 22:1693-1698. 10.1016/j.cub.2012.07.002

Bundesen C. 1990. A theory of visual attention. *Psychol Rev* 97:523-547.

Bundesen C, and Habekost T. 2008. Principles of Visual Attention: Linking Mind and Brain. *Oxford University Press*. 10.1093/acprof:oso/9780198570707.001.0001

Cao B, Mwangi B, Passos IC, Wu MJ, Keser Z, Zunta-Soares GB, Xu DP, Hasan KM, and Soares JC. 2017. Lifespan Gyrification Trajectories of Human Brain in Healthy Individuals and Patients with Major Psychiatric Disorders. *Scientific Reports* 7. ARTN 511

544       10.1038/s41598-017-00582-1

545       Cherubini A, Caligiuri ME, Peran P, Sabatini U, Cosentino C, and Amato F. 2016.

546 Importance of Multimodal MRI in Characterizing Brain Tissue and Its Potential Application

547 for Individual Age Prediction. *Ieee Journal of Biomedical and Health Informatics* 20.

548 10.1109/Jbhi.2016.2559938

549       Cole JH, and Franke K. 2017. Predicting Age Using Neuroimaging: Innovative Brain

550 Ageing Biomarkers. *Trends Neurosci*. 10.1016/j.tins.2017.10.001

551       Cole JH, Marioni RE, Harris SE, and Deary IJ. 2018. Brain age and other bodily 'ages':

552 implications for neuropsychiatry. *Mol Psychiatry*. 10.1038/s41380-018-0098-1

553       Cole JH, Poudel RPK, Tsagkrasoulis D, Caan MWA, Steves C, Spector TD, and

554 Montana G. 2016. Predicting brain age with deep learning from raw imaging data results in a

555 reliable and heritable biomarker. *ARXIV*. 2016arXiv161202572C

556       Cole JH, Ritchie SJ, Bastin ME, Valdes Hernandez MC, Munoz Maniega S, Royle N,

557 Corley J, Pattie A, Harris SE, Zhang Q, Wray NR, Redmond P, Marioni RE, Starr JM, Cox

558 SR, Wardlaw JM, Sharp DJ, and Deary IJ. 2017a. Brain age predicts mortality. *Mol*

559 *Psychiatry*. 10.1038/mp.2017.62

560       Cole JH, Underwood J, Caan MWA, De Francesco D, van Zoest RA, Leech R, Wit

561 FWNM, Portegies P, Geurtsen GJ, Schmand BA, van der Loeff MFS, Franceschi C, Sabin

562 CA, Majoie CBLM, Winston A, Reiss P, Sharp DJ, and Collaboration C. 2017b. Increased

563 brain-predicted aging in treated HIV disease. *Neurology* 88:1349-1357.

564 10.1212/Wnl.0000000000003790

565       Cox SR, Ritchie SJ, Tucker-Drob EM, Liewald DC, Hagenaars SP, Davies G, Wardlaw

566 JM, Gale CR, Bastin ME, and Deary IJ. 2016. Ageing and brain white matter structure in

567 3,513 UK Biobank participants. *Nat Commun* 7:13629. 10.1038/ncomms13629

568       Craik FIM, and Salthouse TA. 2008. *The handbook of aging and cognition*. New York:

569 Psychology Press.

570       Dale AM, Fischl B, and Sereno MI. 1999. Cortical surface-based analysis - I.

571 Segmentation and surface reconstruction. *Neuroimage* 9:179-194. DOI

572 10.1006/nimg.1998.0395

573       Delis DC, Kaplan E, and Kramer JH. 2001. *Delis-Kaplan Executive Function*

574 *System:Technical Manual*. San Antonio, TX: Harcourt Assessment Company.

575       Delis DC, Kramer JH, Kaplan E, and Ober BA. 2000. *California Verbal Learning Test-*

576 *Second Edition (CVLT-II)*. San Antonio, TX: Psychological Corporation.

577    Desikan RS, Segonne F, Fischl B, Quinn BT, Dickerson BC, Blacker D, Buckner RL,
578    Dale AM, Maguire RP, Hyman BT, Albert MS, and Killiany RJ. 2006. An automated labeling
579    system for subdividing the human cerebral cortex on MRI scans into gyral based regions of
580    interest. *Neuroimage* 31:968-980. 10.1016/j.neuroimage.2006.01.021
581    Doan NT, Engvig A, Persson K, Alnaes D, Kaufmann T, Rokicki J, Cordova-Palomera
582    A, Moberget T, Braekhus A, Barca ML, Engedal K, Andreassen OA, Selbaek G, and Westlye
583    LT. 2017. Dissociable diffusion MRI patterns of white matter microstructure and connectivity
584    in Alzheimer's disease spectrum. *Scientific Reports* 7. ARTN 45131
585    10.1038/srep45131
586    Dorum ES, Alnaes D, Kaufmann T, Richard G, Lund MJ, Tonnesen S, Sneve MH,
587    Mathiesen NC, Rustan OG, Gjertsen O, Vatn S, Fure B, Andreassen OA, Nordvik JE, and
588    Westlye LT. 2016. Age-related differences in brain network activation and co-activation
589    during multiple object tracking. *Brain and Behavior* 6. 10.1002/brb3.533
590    Dorum ES, Kaufmann T, Alnaes D, Andreassen OA, Richard G, Kolskar KK, Nordvik
591    JE, and Westlye LT. 2017. Increased sensitivity to age-related differences in brain functional
592    connectivity during continuous multiple object tracking compared to resting-state.
593    *Neuroimage* 148:364-372. 10.1016/j.neuroimage.2017.01.048
594    Espeseth T, Vangkilde SA, Petersen A, Dyrholm M, and Westlye LT. 2014. TVA-based
595    assessment of attentional capacities-associations with age and indices of brain white matter
596    microstructure. *Front Psychol* 5:1177. 10.3389/fpsyg.2014.01177
597    Fischl B, Salat DH, Busa E, Albert M, Dieterich M, Haselgrove C, van der Kouwe A,
598    Killiany R, Kennedy D, Klaveness S, Montillo A, Makris N, Rosen B, and Dale AM. 2002.
599    Whole brain segmentation: Automated labeling of neuroanatomical structures in the human
600    brain. *Neuron* 33:341-355. Doi 10.1016/S0896-6273(02)00569-X
601    Fischl B, van der Kouwe A, Destrieux C, Halgren E, Segonne F, Salat DH, Busa E,
602    Seidman LJ, Goldstein J, Kennedy D, Caviness V, Makris N, Rosen B, and Dale AM. 2004.
603    Automatically parcellating the human cerebral cortex. *Cerebral Cortex* 14:11-22.
604    10.1093/cercor/bhg087
605    Fjell AM, Westlye LT, Grydeland H, Amlien I, Espeseth T, Reinvang I, Raz N, Holland
606    D, Dale AM, Walhovd KB, and Alzheimer Disease Neuroimaging I. 2013. Critical ages in the
607    life course of the adult brain: nonlinear subcortical aging. *Neurobiol Aging* 34:2239-2247.
608    10.1016/j.neurobiolaging.2013.04.006

609    Fox J, and Weisberg S. 2011. An {R} Companion to Applied Regression. In: Second,
610    editor. Thousand Oaks, CA: Sage.
611    Franke K, Gaser C, Manor B, and Novak V. 2013. Advanced BrainAGE in older adults
612    with type 2 diabetes mellitus. *Frontiers in Aging Neuroscience* 5. ARTN 90
613    10.3389/fnagi.2013.00090
614    Gaser C, Franke K, Kloppel S, Koutsouleris N, Sauer H, and Initi AsDN. 2013.
615    BrainAGE in Mild Cognitive Impaired Patients: Predicting the Conversion to Alzheimer's
616    Disease. *PLoS One* 8. ARTN e67346
617    10.1371/journal.pone.0067346
618    Ge Y, Grossman RI, Babb JS, Rabin ML, Mannon LJ, and Kolson DL. 2002. Age-
619    related total gray matter and white matter changes in normal adult brain. Part I: volumetric
620    MR imaging analysis. *AJNR Am J Neuroradiol* 23:1327-1333.
621    Habekost T. 2015. Clinical TVA-based studies: a general review. *Front Psychol* 6:290.
622    10.3389/fpsyg.2015.00290
623    Habekost T, and Starrfelt R. 2009. Visual attention capacity: a review of TVA-based
624    patient studies. *Scand J Psychol* 50:23-32. 10.1111/j.1467-9450.2008.00681.x
625    Habekost T, Vogel A, Rostrup E, Bundesen C, Kyllingsbaek S, Garde E, Ryberg C, and
626    Waldemar G. 2013. Visual processing speed in old age. *Scand J Psychol* 54:89-94.
627    10.1111/sjop.12008
628    Habes M, Guray E, Toledo JB, Zhang T, Bryan RN, Janowitz D, Doshi J, von
629    Sarnowski B, Hegenscheid K, Voelzke H, Schminke U, Hoffmann W, Grabe HJ, and
630    Davatzikos C. 2016. Non-Resilient Brain Aging in Association with Cardiovascular Risk and
631    White Matter Hyperintensities: The Ship Study. *Alzheimer's & Dementia* 12:P226-P227.
632    10.1016/j.jalz.2016.06.407
633    Han CE, Peraza LR, Taylor JP, and Kaiser M. 2014. Predicting Age across Human
634    Lifespan Based on Structural Connectivity from Diffusion Tensor Imaging. *2014 Ieee*
635    *Biomedical Circuits and Systems Conference (Biocas)*:137-140.
636    Harada CN, Natelson Love MC, and Triebel KL. 2013. Normal cognitive aging. *Clin*
637    *Geriatr Med* 29:737-752. 10.1016/j.cger.2013.07.002
638    Hastie T. 2017. gam: Generalized Additive Models.
639    Hua K, Zhang JY, Wakana S, Jiang HY, Li X, Reich DS, Calabresi PA, Pekar JJ, van
640    Zijl PCM, and Mori S. 2008. Tract probability maps in stereotaxic spaces: Analyses of white

641    matter anatomy and tract-specific quantification. *Neuroimage* 39:336-347.

642    10.1016/j.neuroimage.2007.07.053

643    Kaufmann T, van der Meer D, Doan NT, Schwarz E, Lund MJ, Agartz I, Alnæs D,

644    Barch DM, Baur-Streubel R, Bertolino A, Bettella F, Beyer MK, Bøen E, Borgwardt S,

645    Brandt CL, Buitelaar J, Celius EG, Cervenka S, Conzelmann A, Córdova-Palomera A, Dale

646    AM, de Quervain DJF, Di Carlo P, Djurovic S, Dørum ES, Eisenacher S, Elvsashagen T,

647    Espeseth T, Fatouros-Bergman H, Flyckt L, Franke B, Frei O, Haatveit B, Haberg AK, Harbo

648    HF, Hartman CA, Heslenfeld D, Hoekstra PJ, Høgestøl EA, Jernigan T, Jonassen R, Jönsson

649    EG, Kirsch P, Kloszewska I, Kolskar K-K, Landrø NI, Le Hellard S, Lesch K-P, Lovestone S,

650    Lundervold A, Lundervold AJ, Maglanoc LA, Malt UF, Mecocci P, Melle I, Meyer-

651    Lindenberg A, Moberget T, Norbom LB, Nordvik JE, Nyberg L, Oosterlaan J, Papalino M,

652    Papassotiropoulos A, Pauli P, Pergola G, Persson K, Richard G, Rokicki J, Sanders A-M,

653    Selbæk G, Shadrin AA, Smeland OB, Soininen H, Sowa P, Steen VM, Tsolaki M, Ulrichsen

654    KM, Vellas B, Wang L, Westman E, Ziegler GC, Zink M, Andreassen OA, and Westlye LT.

655    2018. Genetics of brain age suggest an overlap with common brain disorders. *bioRxiv*.

656    Kuhn T, Kaufmann T, Doan NT, Westlye LT, Jones J, Nunez RA, Bookheimer SY,

657    Singer EJ, Hinkin CH, and Thames AD. 2018. An augmented aging process in brain white

658    matter in HIV. *Hum Brain Mapp*. 10.1002/hbm.24019

659    Liem F, Varoquaux G, Kynast J, Beyer F, Masouleh SK, Huntenburg JM, Lampe L,

660    Rahim M, Abraham A, Craddock RC, Riedel-Heller S, Luck T, Loeffler M, Schroeter ML,

661    Witte AV, Villringer A, and Margulies DS. 2017. Predicting brain-age from multimodal

662    imaging data captures cognitive impairment. *Neuroimage* 148:179-188.

663    10.1016/j.neuroimage.2016.11.005

664    Liu K, Yao S, Chen K, Zhang J, Yao L, Li K, Jin Z, and Guo X. 2017. Structural Brain

665    Network Changes across the Adult Lifespan. *Front Aging Neurosci* 9:275.

666    10.3389/fnagi.2017.00275

667    Madan CR, and Kensinger EA. 2018. Predicting age from cortical structure across the

668    lifespan. *Eur J Neurosci* 47:399-416. 10.1111/ejn.13835

669    Marquand AF, Rezek I, Buitelaar J, and Beckmann CF. 2016. Understanding

670    Heterogeneity in Clinical Cohorts Using Normative Models: Beyond Case-Control Studies.

671    *Biol Psychiatry* 80:552-561. 10.1016/j.biopsych.2015.12.023

672    McAvinue LP, Habekost T, Johnson KA, Kyllingsbaek S, Vangkilde S, Bundesen C,

673    and Robertson IH. 2012. Sustained attention, attentional selectivity, and attentional capacity

674    across the lifespan. *Atten Percept Psychophys* 74:1570-1582. 10.3758/s13414-012-0352-6

675    Mori S, Wakana S, van Zijl PCM, and Nagae-Poetscher LM. 2005. MRI Atlas of

676    Human White Matter. In: Science E, editor. 1st Edition ed: Elsevier Science. p 276.

677    Müllner D. 2013. {fastcluster}: Fast Hierarchical, Agglomerative Clustering Routines

678    for {R} and {Python}. *Journal of Statistical Software* 53:1-18.

679    Nasreddine ZS, Phillips NA, Bedirian V, Charbonneau S, Whitehead V, Collin I,

680    Cummings JL, and Chertkow H. 2005. The montreal cognitive assessment, MoCA: A brief

681    screening tool for mild cognitive impairment. *Journal of the American Geriatrics Society*

682    53:695-699. DOI 10.1111/j.1532-5415.2005.53221.x

683    Raz N, Ghisletta P, Rodrigue KM, Kennedy KM, and Lindenberger U. 2010.

684    Trajectories of brain aging in middle-aged and older adults: regional and individual

685    differences. *Neuroimage* 51:501-511. 10.1016/j.neuroimage.2010.03.020

686    Ronan L, Alexander-Bloch AF, Wagstyl K, Farooqi S, Brayne C, Tyler LK, Fletcher

687    PC, and Cam-CAN. 2016. Obesity associated with increased brain age from midlife.

688    *Neurobiology of Aging* 47:63-70. 10.1016/j.neurobiolaging.2016.07.010

689    Salat DH, Tuch DS, Greve DN, van der Kouwe AJW, Hevelone ND, Zaleta AK, Rosen

690    BR, Fischl B, Corkin S, Rosas HD, and Dale AM. 2005. Age-related alterations in white

691    matter microstructure measured by diffusion tensor imaging. *Neurobiology of Aging* 26:1215-

692    1227. 10.1016/j.neurobiolaging.2004.09.017

693    Schnack HG, van Haren NE, Nieuwenhuis M, Hulshoff Pol HE, Cahn W, and Kahn RS.

694    2016. Accelerated Brain Aging in Schizophrenia: A Longitudinal Pattern Recognition Study.

695    *Am J Psychiatry* 173:607-616. 10.1176/appi.ajp.2015.15070922

696    Shafto MA, Tyler LK, Dixon M, Taylor JR, Rowe JB, Cusack R, Calder AJ, Marslen-

697    Wilson WD, Duncan J, Dalgleish T, Henson RN, Brayne C, Matthews FE, and Cam-CAN.

698    2014. The Cambridge Centre for Ageing and Neuroscience (Cam-CAN) study protocol: a

699    cross-sectional, lifespan, multidisciplinary examination of healthy cognitive ageing. *Bmc*

700    *Neurology* 14. ARTN 204

701    10.1186/s12883-014-0204-1

702    Smith SM, Jenkinson M, Johansen-Berg H, Rueckert D, Nichols TE, Mackay CE,

703    Watkins KE, Ciccarelli O, Cader MZ, Matthews PM, and Behrens TEJ. 2006. Tract-based

704    spatial statistics: Voxelwise analysis of multi-subject diffusion data. *Neuroimage* 31:1487-

705    1505. 10.1016/j.neuroimage.2006.02.024

706        Smith SM, Jenkinson M, Woolrich MW, Beckmann CF, Behrens TEJ, Johansen-Berg

707    H, Bannister PR, De Luca M, Drobnjak I, Flitney DE, Niazy RK, Saunders J, Vickers J,

708    Zhang YY, De Stefano N, Brady JM, and Matthews PM. 2004. Advances in functional and

709    structural MR image analysis and implementation as FSL. *Neuroimage* 23:S208-S219.

710    10.1016/j.neuroimage.2004.07.051

711        Sperling G. 1960. The information available in brief visual presentations. *Psychological*

712    *Monographs: General and Applied* 74:1-29. 10.1037/h0093759

713        Steffener J, Habeck C, O'Shea D, Razlighi Q, Bherer L, and Stern Y. 2016. Differences

714    between chronological and brain age are related to education and self-reported physical

715    activity. *Neurobiology of Aging* 40:138-144. 10.1016/j.neurobiolaging.2016.01.014

716        Storsve AB, Fjell AM, Tamnes CK, Westlye LT, Overbye K, Aasland HW, and

717    Walhovd KB. 2014. Differential Longitudinal Changes in Cortical Thickness, Surface Area

718    and Volume across the Adult Life Span: Regions of Accelerating and Decelerating Change.

719    *Journal of Neuroscience* 34:8488-8498. 10.1523/Jneurosci.0391-14.2014

720        Taylor JR, Williams N, Cusack R, Auer T, Shafto MA, Dixon M, Tyler LK, Cam C,

721    and Henson RN. 2017. The Cambridge Centre for Ageing and Neuroscience (Cam-CAN) data

722    repository: Structural and functional MRI, MEG, and cognitive data from a cross-sectional

723    adult lifespan sample. *Neuroimage* 144:262-269. 10.1016/j.neuroimage.2015.09.018

724        Valizadeh SA, Hanggi J, Merillat S, and Jancke L. 2017. Age prediction on the basis of

725    brain anatomical measures. *Hum Brain Mapp* 38:997-1008. 10.1002/hbm.23434

726        Wakana S, Caprihan A, Panzenboeck MM, Fallon JH, Perry M, Gollub RL, Hua KG,

727    Zhang JY, Jiang HY, Dubey P, Blitz A, van Zijl P, and Mori S. 2007. Reproducibility of

728    quantitative tractography methods applied to cerebral white matter. *Neuroimage* 36:630-644.

729    10.1016/j.neuroimage.2007.02.049

730        Warnes GR, Bolker B, Bonebakker L, Gentleman R, Liaw WHA, Lumley T, Maechler

731    M, Magnusson A, Moeller S, Schwartz M, and Venables B. 2016. gplots: Various R

732    Programming Tools for Plotting Data.

733        Wechsler D. 1999. *Wechsler Abbreviated Scale of Intelligence (WASI)*: Psychological

734    Corporation.

735        Westlye LT, Walhovd KB, Dale AM, Bjornerud A, Due-Tonnessen P, Engvig A,

736    Grydeland H, Tamnes CK, Ostby Y, and Fjell AM. 2010a. Differentiating maturational and

737     aging-related changes of the cerebral cortex by use of thickness and signal intensity.

738     *Neuroimage* 52:172-185. 10.1016/j.neuroimage.2010.03.056

739     Westlye LT, Walhovd KB, Dale AM, Bjornerud A, Due-Tonnessen P, Engvig A,

740     Grydeland H, Tamnes CK, Ostby Y, and Fjell AM. 2010b. Life-Span Changes of the Human

741     Brain White Matter: Diffusion Tensor Imaging (DTI) and Volumetry. *Cerebral Cortex*

742     20:2055-2068. 10.1093/cercor/bhp280

743     Wiegand I, Lauritzen MJ, Osler M, Mortensen EL, Rostrup E, Rask L, Richard N,

744     Horwitz A, Benedek K, Vangkilde S, and Petersen A. 2018. EEG correlates of visual short-

745     term memory in older age vary with adult lifespan cognitive development. *Neurobiol Aging*

746     62:210-220. 10.1016/j.neurobiolaging.2017.10.018

747     Willer L, Pedersen PM, Forchhammer HB, and Christensen HK. 2016. Cognitive

748     assessment at bedside for iPad: A preliminary validation of a novel cognitive test for stroke

749     patients. *European Stroke Journal* 1:294-301. 10.1177/2396987316665233

750     Wolfers T, Doan NT, Kaufmann T, Alnæs D, Moberget T, Agartz I, Buitelaar J, Ueland

751     T, Melle I, Beckmann CF, Franke B, Andreassen OA, Westlye LT, and Marquand A. in press.

752     Extensive interindividual differences in schizophrenia and bipolar disorder: mapping

753     biological heterogeneity in reference to normative brain ageing *JAMA Psychiatry*.

754     Wright SP. 1992. Adjusted P-Values for Simultaneous Inference. *Biometrics* 48:1005-

755     1013. Doi 10.2307/2532694

756

757

758

759

760

761

762

763

764

765

766

767

768

769

770    **Figure legends**

771    **Fig. 1** Histogram of the age distribution for each sample.

772

773    **Fig. 2** Comparison between the 11 BAG models. (a) Heatmap of the correlation between

774    different BAGs. (b) Correlations between the chronological age and the predicted age in the

775    test sample for each model with their confidence intervals. (c) Mean and standard error of the

776    45 p-values ($-\log_{10}(p)$) for the cognitive scores and composite scores for each row (i.e.

777    BAGs), with a higher mean representing a stronger global association across tests. (d)

778    Correlation between the chronological age of each subjects and the combined age, (e) the

779    brain morphometry age, and (f) the white matter microstructure age.

780

781    **Fig. 3** Hierarchical clustering of the cognitive features. Each cognitive score was normalized

782    and when required the scores were multiplied by -1 to ensure that positive scores represent

783    good performance. The higher panel shows the dendrogram resulting from the hierarchical

784    clustering of the scores in 7 cognitive domains.

785

786    **Fig. 4** Heatmap of the association between cognitive scores and brain age gaps. The color

787    scale depicts the minus log of the p-values ($-\log_{10}(p)$) for each association. The association

788    marked with a small star represents significant associations after FDR correction, and the one

789    marked with a big star shows significant associations after Bonferroni correction.

790

791    **Fig. 5** Scatter plots of the 2 strongest associations between cognitive measures and BAG. The

792    color gradient represents the age where lighter color is assigned to older individuals, and

793    darker color to younger individuals. All associations indicate worse performance with higher

794    brain age gap.

795

796

797

798

799

800

801

802 **Table legends**

803 **Table 1.** Demographics and cognitive information. * significant associations between

804 cognitive measures with age after FDR correction, ** significant associations between

805 cognitive measures with age after Bonferroni correction

806

807 **Table 2.** Cognitive associations with Brain Age Gap (BAG) – statistics. * FDR significant **

808 Bonferroni significant

809

810

811

812 **Supplementary Materials**

813 **Fig. S1.** Heatmap of the association between cognitive scores and brain age gaps using non-

814 linear models, including age, age$^2$ and sex as covariates. The color scale depicts the minus log

815 of the p-values ($-\log_{10}(p)$) for each association. The association marked with a small star

816 represents significant associations after FDR correction, and the one marked with a big star

817 shows significant associations after Bonferroni correction.

818

819 **Table S1.** Cognitive associations with Brain Age Gap (BAG) using non-linear models,

820 including age, age$^2$ and sex as covariates – statistics. * FDR significant ** Bonferroni

821 significant.

822

823

824

825

826

827

828

829

830

831

832

833

834

835 **Tables**

836 Demographics and cognitive information

| | Cam-CAN | StrokeMRI Mean (SD) | Range (IQR) | Main effect Age $t$ ($p$) | Main effect Sex $t$ ($p$) |
|---|---|---|---|---|---|
| Total N (% females) | 612 (51.3%) | 265 (63.4%) | | | |
| Mean age (SD) | 54.41 (18.26) | 56.95 (14.84) | | | |
| Age range | 18-87 | 20-88 | | | |
| MoCA | - | 27.60 (1.72) | 21 – 30 (2) | -4.57 (<0.001)** | -2.32 (0.021) |
| WASI words | - | 65.27 (6.60) | 44 – 79 (10) | 4.72 (<0.001)** | 0.10 (0.920) |
| WASI matrix | - | 25.39 (5.64) | 7 – 35 (6) | -7.60 (<0.001)** | -0.28 (0.776) |
| CVLT learning 1-5 | - | 48.92 (11.37) | 17 – 73 (15.5) | -5.05 (<0.001)** | -5.26 (<0.001) |
| CVLT interference | - | 5.53 (2.15) | 0 – 13 (3) | -4.33 (<0.001)** | -0.41 (0.681) |
| CVLT recall | - | 10.83 (3.42) | 0 – 16 (5) | -6.50 (<0.001)** | 5.94 (<0.001) |
| CVLT delayed recall | - | 11.39 (3.44) | 0 – 16 (5) | -4.97 (<0.001)** | -5.51 (<0.001) |
| CVLT recognition hit | - | 14.70 (1.50) | 8 – 16 (2) | -2.62 (0.0093)* | -2.68 (0.008) |
| CVLT recognition errors | - | 3.79 (3.92) | 0 – 18 (4) | 5.22 (<0.001)** | 4.18 (<0.001) |
| CVLT recog misses | - | 1.30 (1.49) | 0 – 8 (2) | 2.62 (0.0093)* | 2.68 (0.008) |
| CVLT recog false alarm | - | 2.46 (3.48) | 0 – 18 (3) | 4.45 (<0.001)** | 3.59 (0.0004) |
| CVLT recog correct rejection | - | 44.20 (3.92) | 30 – 48 (4) | -5.22 (<0.001)** | -4.18 (<0.001) |
| CVLT d' | - | 2.97 (0.72) | 0.97 – 3.90 (1.11) | -5.01 (<0.001)** | -4.50 (<0.001) |
| STROOP 1 | - | 31.14 (5.66) | 21 – 50 (7) | 5.05 (<0.001)** | 2.44 (0.015) |
| STROOP 2 | - | 22.12 (3.49) | 14 – 35 (4) | 2.89 (0.004)* | 2.27 (0.024) |
| STROOP 3 | - | 55.86 (14.13) | 10 – 108 (15) | 7.55 (<0.001)** | 2.97 (0.003) |
| STROOP 4 | - | 61.74 (14.85) | 33 – 117 (19) | 7.51 (<0.001)** | 1.77 (0.078) |
| STROOP mean 1 and 2 | - | 26.54 (4.16) | 18.5 – 42 (5) | 4.47 (<0.001)** | 2.47 (0.014) |
| STROOP 3 minus mean 1 and 2 | - | 81.94 (16.51) | 34.5 – 145 (18.5) | 7.31 (<0.001)** | 3.02 (0.003) |
| STROOP 4 minus mean 1 and 2 | - | 87.64 (16.73) | 53.5 – 142 (24) | 7.52 (<0.001)** | 1.85 (0.066) |
| CP – Right motor speed | - | 79.56 (23.34) | 34 – 153 (32) | -12.25 (<0.001)** | -0.36 (0.716) |
| CP – Left motor speed | - | 81.36 (17.80) | 39 – 131 (26) | -12.07 (<0.001)** | 0.20 (0.842) |
| CP – FAS Phonological flow | - | 54.70 (14.53) | 14 – 95 (19.75) | -0.61 (0.541) | -2.58 (0.011) |
| CP – FAS Semantic flow | - | 51.00 (10.14) | 27 – 81 (13) | -2.93 (0.004)* | -3.93 (<0.001) |

| | | | | | |
|---|---|---|---|---|---|
| CP – Visual WM forward ls | - | 4.23 (1.01) | 2 – 7 (2) | -5.31 (<0.001)** | 0.29 (0.774) |
| CP – Visual WM forward ss | - | 5.45 (1.87) | 1 – 10 (3) | -6.59 (<0.001)** | -0.25 (0.803) |
| CP – Visual WM backward ls | - | 3.80 (1.28) | 0 – 8 (1) | -4.60 (<0.001)** | -1.85 (0.065) |
| CP – Visual WM backward ss | - | 4.56 (2.08) | 0 – 12 (3) | -5.48 (<0.001)** | -1.02 (0.309) |
| CP – Visual WM ss | - | 9.96 (3.57) | 1 – 21 (4) | -7.04 (<0.001)** | -0.95 (0.342) |
| CP – Spatial stroop congruent (ms) | - | 674.42 (132.77) | 410 – 1159 (181) | 8.52 (<0.001)** | -1.03 (0.304) |
| CP – Spatial stroop incongruent (ms) | - | 929.52 (198.01) | 462 – 1827 (269) | 9.41 (<0.001)** | -0.75 (0.451) |
| CP – Spatial stroop Errors | - | 2.17 (2.41) | 0 – 11 (3) | 0.73 (0.463) | 1.59 (0.113) |
| CP – Spatial stroop numb of reps | - | 119.63 (16.64) | 55 – 166 (22) | -9.67 (<0.001)** | 1.23 (0.219) |
| CP – Spatial stroop incong – cong (ms) | - | 252 (110) | 20 – 678 (134.5) | 5.73 (<0.001)** | -0.68 (0.498) |
| CP – Spatspan ls | - | 5.37 (1.78) | 1 – 10 (2) | -9.12 (<0.001)** | -4.88 (<0.001) |
| CP – Spatspan tot | - | 29.87 (12.43) | 3 – 55 (18) | -9.28 (<0.001)** | -4.66 (<0.001) |
| CP – Coding corr | - | 54.50 (12.11) | 24 – 88 (16) | -16.69 (<0.001)** | -2.46 (0.015) |
| CP – Coding error | - | 0.67 (0.99) | 0 – 5 (1) | -1.10 (0.271) | 1.56 (0.121) |
| TVA – Short-term memory storage ($K$) | - | 3.38 (0.77) | 1.46 – 5.53 (1.09) | -7.75 (<0.001)** | -1.52 (0.129) |
| TVA – Processing speed ($C$) | - | 31.55 (14.07) | 5.99 – 89.67 (14.75) | -4.69 (<0.001)** | 0.41 (0.6847) |
| TVA – Perceptual threshold ($t_0$) | - | 23.01 (14.05) | 0 – 79.75 (17.59) | 5.72 (<0.001)** | -1.94 (0.053) |
| TVA – Error rate | - | 0.10 (0.06) | 0.0035 – 0.3316 (0.0983) | -1.35 (0.177) | 0.67 (0.502) |
| Cluster 1 | - | - | - | -7.19 (<0.001)** | -5.16 (<0.001) |
| Cluster 2 | - | - | - | -7.28 (<0.001)** | 1.61 (0.110) |
| Cluster 3 | - | - | - | -2.01 (0.045)* | -3.99 (<0.001) |
| Cluster 4 | - | - | - | -9.98 (<0.001)** | 1.25 (0.212) |
| Cluster 5 | - | - | - | -6.86 (<0.001)** | -2.56 (0.011) |
| Cluster 6 | - | - | - | -15.79 (<0.001)** | -1.08 (0.282) |
| Cluster 7 | - | - | - | -6.50 (<0.001)** | -0.77 (0.440) |

837    Table 1. Demographics and cognitive information. * significant associations between

838    cognitive measures with age after FDR correction, ** significant associations between

839    cognitive measures with age after Bonferroni correction

840

841

842

843 Cognitive associations with Brain Age Gap (BAG) – statistics

| Test | Adj $R^2$ no-BAG | BAG | Main effect Age $t\ (p)$ | Main effect Sex $t\ (p)$ | Main effect BAG $t\ (p)$ | Adj $R^2$ |
|---|---|---|---|---|---|---|
| MoCA | 0.0907 | T1 | -4.5596 (<0.001) | -2.3145 (0.021) | -0.124 (0.901) | 0.0878 |
| | | DTI | -4.5599 (<0.001) | -2.3155 (0.021) | 1.5914 (0.113) | 0.0966 |
| | | Combined | -4.5653 (<0.001) | -2.3176 (0.021) | -0.4626 (0.644) | 0.0885 |
| WASI words | 0.0731 | T1 | 4.7118 (<0.001) | 0.1020 (0.919) | -0.2169 (0.828) | 0.0704 |
| | | DTI | 4.7056 (<0.001) | 0.1121 (0.911) | -0.8126 (0.417) | 0.0727 |
| | | Combined | 4.7091 (<0.001) | 0.1041 (0.917) | -0.4827 (0.630) | 0.0711 |
| WASI matrix | 0.1791 | T1 | -7.6061 (<0.001) | -0.2785 (0.781) | -0.9158 (0.361) | 0.1793 |
| | | DTI | -7.6610 (<0.001) | -0.2624 (0.793) | -1.6546 (0.099) | 0.1854 |
| | | Combined | -7.6128 (<0.001) | -0.2726 (0.785) | -1.1102 (0.268) | 0.1806 |
| CVLT learning 1-5 | 0.1810 | T1 | -5.0373 (<0.001) | -5.2514 (<0.001) | -0.2505 (0.802) | 0.1750 |
| | | DTI | -5.0418 (<0.001) | -5.2533 (<0.001) | -0.3608 (0.719) | 0.1753 |
| | | Combined | -5.0387 (<0.001) | -5.2522 (<0.001) | -0.2492 (0.803) | 0.1750 |
| CVLT interference | 0.0664 | T1 | -4.3256 (<0.001) | -0.4062 (0.685) | -0.9588 (0.339) | 0.0626 |
| | | DTI | -4.3218 (<0.001) | -0.4104 (0.682) | -0.2391 (0.811) | 0.0594 |
| | | Combined | -4.3202 (<0.001) | -0.4101 (0.682) | -0.1875 (0.851) | 0.0594 |
| CVLT recall | 0.2438 | T1 | -6.4897 (<0.001) | -5.9257 (<0.001) | -0.4868 (0.627) | 0.2397 |
| | | DTI | -6.4885 (<0.001) | -5.9257 (<0.001) | -0.1245 (0.901) | 0.2391 |
| | | Combined | -6.5080 (<0.001) | -5.9373 (<0.001) | -1.1114 (0.268) | 0.2427 |
| CVLT delayed recall | 0.1850 | T1 | -4.9636 (<0.001) | -5.4973 (<0.001) | 0.1421 (0.887) | 0.1808 |
| | | DTI | -4.9611 (<0.001) | -5.4969 (<0.001) | 0.224 (0.823) | 0.1809 |
| | | Combined | -4.9655 (<0.001) | -5.4954 (<0.001) | -0.3038 (0.762) | 0.1810 |
| CVLT recognition hits | 0.0494 | T1 | -2.6125 (0.010) | -2.6822 (0.008) | -0.8586 (0.391) | 0.0486 |
| | | DTI | -2.6144 (0.010) | -2.6786 (0.008) | 0.0946 (0.925) | 0.0459 |
| | | Combined | -2.6212 (0.009) | -2.6854 (0.008) | -1.0724 (0.285) | 0.0501 |
| CVLT recognition errors | 0.1526 | T1 | 5.2227 (<0.001) | 4.1850 (<0.001) | -0.8471 (0.398) | 0.1528 |
| | | DTI | 5.2115 (<0.001) | 4.1755 (<0.001) | -0.5651 (0.573) | 0.1514 |
| | | Combined | 5.2139 (<0.001) | 4.1740 (<0.001) | -0.2537 (0.800) | 0.1506 |
| CVLT recog misses | 0.0494 | T1 | 2.6125 (0.010) | 2.6822 (0.008) | 0.8586 (0.391) | 0.0486 |
| | | DTI | 2.6144 (0.010) | 2.6786 (0.008) | -0.0946 (0.925) | 0.0459 |
| | | Combined | 2.6212 (0.009) | 2.6854 (0.008) | 1.0724 (0.285) | 0.0501 |
| CVLT recog false alarm | 0.1150 | T1 | 4.4519 (<0.001) | 3.5827 (<0.001) | -0.776 (0.439) | 0.1146 |
| | | DTI | 4.4378 (<0.001) | 3.5803 (<0.001) | -0.5207 (0.603) | 0.1134 |
| | | Combined | 4.4418 (<0.001) | 3.5788 (<0.001) | -0.3488 (0.728) | 0.1129 |
| CVLT recog correct rejection | 0.1526 | T1 | -5.2227 (<0.001) | -4.1850 (<0.001) | 0.8471 (0.398) | 0.1528 |
| | | DTI | -5.2115 (<0.001) | -4.1755 (<0.001) | 0.5651 (0.573) | 0.1514 |
| | | Combined | -5.2139 (<0.001) | -4.1740 (<0.001) | 0.2537 (0.800) | 0.1506 |
| CVLT d' | 0.1566 | T1 | -5.0074 (<0.001) | -4.4914 (<0.001) | 0.3628 (0.717) | 0.1536 |
| | | DTI | -5.0021 (<0.001) | -4.4969 (<0.001) | 0.8538 (0.394) | 0.1556 |
| | | Combined | -5.0038 (<0.001) | -4.4902 (<0.001) | 0.1699 (0.865) | 0.1533 |
| STROOP 1 | 0.1118 | T1 | 5.1466 (<0.001) | 2.4999 (0.013) | 2.6939 (0.008) | 0.1299 |

|  |  |  |  |  |  |  |
|---|---|---|---|---|---|---|
|  |  | DTI | 5.0968 (<0.001) | 2.4769 (0.014) | 1.6664 (0.097) | 0.1147 |
|  |  | Combined | 5.2111 (<0.001) | 2.5317 (0.012) | 3.3767 (<0.001)* | 0.1434 |
| STROOP 2 | 0.0477 | T1 | 2.8868 (0.004) | 2.2619 (0.025) | 0.1557 (0.876) | 0.0433 |
|  |  | DTI | 2.8768 (0.004) | 2.2489 (0.025) | -0.4639 (0.643) | 0.0440 |
|  |  | Combined | 2.8949 (0.004) | 2.2713 (0.024) | 0.4976 (0.619) | 0.0442 |
| STROOP 3 | 0.2104 | T1 | 7.5930 (<0.001) | 2.9898 (0.003) | 1.5092 (0.133) | 0.2109 |
|  |  | DTI | 7.6511 (<0.001) | 3.0224 (0.003) | 2.231 (0.027) | 0.2190 |
|  |  | Combined | 7.6793 (<0.001) | 3.0233 (0.003) | 2.5768 (0.011) | 0.2240 |
| STROOP 4 | 0.1887 | T1 | 7.5403 (<0.001) | 1.7884 (0.075) | 1.2397 (0.216) | 0.1906 |
|  |  | DTI | 7.5847 (<0.001) | 1.8121 (0.071) | 1.7368 (0.084) | 0.1953 |
|  |  | Combined | 7.6387 (<0.001) | 1.8247 (0.069) | 2.3662 (0.019) | 0.2033 |
| STROOP mean 1 and 2 | 0.0949 | T1 | 4.5089 (<0.001) | 2.5033 (0.013) | 1.5875 (0.114) | 0.0978 |
|  |  | DTI | 4.4750 (<0.001) | 2.4760 (0.014) | 0.3927 (0.695) | 0.0894 |
|  |  | Combined | 4.5432 (<0.001) | 2.5399 (0.012) | 2.0254 (0.044) | 0.1034 |
| STROOP 3 minus mean 1 and 2 | 0.2051 | T1 | 7.3383 (<0.001) | 3.0427 (0.003) | 1.1397 (0.256) | 0.2021 |
|  |  | DTI | 7.3613 (<0.001) | 3.0703 (0.002) | 1.3546 (0.177) | 0.2038 |
|  |  | Combined | 7.4197 (<0.001) | 3.1063 (0.002) | 2.1881 (0.030) | 0.2130 |
| STROOP 4 minus mean 1 and 2 | 0.1936 | T1 | 7.5360 (<0.001) | 1.8671 (0.063) | 0.8763 (0.382) | 0.1919 |
|  |  | DTI | 7.5297 (<0.001) | 1.8697 (0.063) | 0.6331 (0.527) | 0.1907 |
|  |  | Combined | 7.6081 (<0.001) | 1.9215 (0.056) | 1.7531 (0.081) | 0.1993 |
| CP – Right motor speed | 0.3695 | T1 | -12.2893 (<0.001) | -0.3592 (0.720) | -1.5504 (0.122) | 0.3676 |
|  |  | DTI | -12.2318 (<0.001) | -0.3612 (0.718) | -0.3435 (0.732) | 0.3620 |
|  |  | Combined | -12.3125 (<0.001) | -0.3587 (0.720) | -1.8139 (0.071) | 0.3697 |
| CP – Left motor speed | 0.3630 | T1 | -12.1437 (<0.001) | 0.2100 (0.834) | -1.9945 (0.047) | 0.3634 |
|  |  | DTI | -12.0669 (<0.001) | 0.2081 (0.835) | -0.8704 (0.385) | 0.3555 |
|  |  | Combined | -12.2516 (<0.001) | 0.2149 (0.830) | -2.9047 (0.004) | 0.3740 |
| CP – FAS Semantic flow | 0.0840 | T1 | -2.9562 (0.003) | -3.9454 (<0.001) | -2.0826 (0.038) | 0.0960 |
|  |  | DTI | -2.9607 (0.003) | -3.9388 (<0.001) | -2.0997 (0.037) | 0.0963 |
|  |  | Combined | -2.9513 (0.004) | -3.9389 (<0.001) | -1.8308 (0.068) | 0.0926 |
| CP – Visual WM forward ls | 0.0936 | T1 | -5.3071 (<0.001) | 0.2850 (0.776) | -0.5838 (0.560) | 0.0906 |
|  |  | DTI | -5.3392 (<0.001) | 0.2963 (0.767) | -1.7204 (0.087) | 0.0999 |
|  |  | Combined | -5.3059 (<0.001) | 0.2853 (0.776) | -0.3127 (0.755) | 0.0897 |
| CP – Visual WM forward ss | 0.1416 | T1 | -6.5795 (<0.001) | -0.2502 (0.803) | -0.2158 (0.829) | 0.1375 |
|  |  | DTI | -6.6000 (<0.001) | -0.2448 (0.807) | -1.1695 (0.243) | 0.1420 |
|  |  | Combined | -6.5786 (<0.001) | -0.2496 (0.803) | -0.02 (0.984) | 0.1373 |
| CP – Visual WM backward ls | 0.0852 | T1 | -4.5941 (<0.001) | -1.8511 (0.065) | -0.1047 (0.917) | 0.0820 |
|  |  | DTI | -4.6170 (<0.001) | -1.8545 (0.065) | -1.3334 (0.184) | 0.0884 |
|  |  | Combined | -4.6051 (<0.001) | -1.8550 (0.065) | -0.8013 (0.424) | 0.0843 |
| CP – Visual WM backward ss | 0.1022 | T1 | -5.4741 (<0.001) | -1.0181 (0.310) | -0.2721 (0.786) | 0.1015 |
|  |  | DTI | -5.4971 (<0.001) | -1.0179 (0.310) | -1.3043 (0.193) | 0.1072 |
|  |  | Combined | -5.4898 (<0.001) | -1.0215 (0.308) | -1.0074 (0.315) | 0.1048 |
| CP – Visual WM ss | 0.1607 | T1 | -7.0322 (<0.001) | -0.9515 (0.342) | -0.3013 (0.763) | 0.1591 |
|  |  | DTI | -7.0622 (<0.001) | -0.9511 (0.342) | -1.3634 (0.174) | 0.1649 |

| | | | | | | |
|---|---|---|---|---|---|---|
| | | Combined | -7.0399 (<0.001) | -0.9528 (0.342) | -0.6665 (0.506) | 0.1603 |
| CP – Spatial stroop congruent | 0.2288 | T1 | 8.6156 (<0.001) | -1.0080 (0.314) | 2.1921 (0.029) | 0.2288 |
| | | DTI | 8.6687 (<0.001) | -1.0021 (0.317) | 2.6995 (0.007) | 0.2362 |
| | | Combined | 8.8278 (<0.001) | -0.9828 (0.327) | 3.9007 (<0.001)** | 0.2588 |
| CP – Spatial stroop incongruent | 0.2548 | T1 | 9.5489 (<0.001) | -0.7429 (0.458) | 2.6569 (0.008) | 0.2700 |
| | | DTI | 9.5931 (<0.001) | -0.7587 (0.449) | 2.8817 (0.004) | 0.2735 |
| | | Combined | 9.7197 (<0.001) | -0.7378 (0.461) | 3.8071 (<0.001)** | 0.2903 |
| CP – Spatial stroop numb of reps | 0.2731 | T1 | -9.7755 (<0.001) | 1.2211 (0.223) | -2.2212 (0.027) | 0.2753 |
| | | DTI | -9.8507 (<0.001) | 1.2328 (0.219) | -2.9614 (0.003) | 0.2859 |
| | | Combined | -9.9891 (<0.001) | 1.2198 (0.224) | -3.8816 (<0.001)** | 0.3027 |
| CP – Spatial stroop incong – cong | 0.1012 | T1 | 5.7663 (<0.001) | -0.6595 (0.510) | 1.5611 (0.120) | 0.1134 |
| | | DTI | 5.7466 (<0.001) | -0.6678 (0.505) | 0.9705 (0.333) | 0.1081 |
| | | Combined | 5.7568 (<0.001) | -0.6584 (0.511) | 1.2056 (0.229) | 0.1099 |
| CP – Spatspan ls | 0.3055 | T1 | -9.1038 (<0.001) | -4.8656 (<0.001) | -0.032 (0.975) | 0.3009 |
| | | DTI | -9.1746 (<0.001) | -4.9104 (<0.001) | -1.5749 (0.117) | 0.3077 |
| | | Combined | -9.1043 (<0.001) | -4.8663 (<0.001) | -0.075 (0.940) | 0.3009 |
| CP – Spatspan total | 0.3057 | T1 | -9.2664 (<0.001) | -4.6439 (<0.001) | 0.1074 (0.915) | 0.3024 |
| | | DTI | -9.3260 (<0.001) | -4.6815 (<0.001) | -1.3773 (0.170) | 0.3076 |
| | | Combined | -9.2686 (<0.001) | -4.6461 (<0.001) | -0.0612 (0.951) | 0.3024 |
| CP – Coding corr | 0.5387 | T1 | -16.7647 (<0.001) | -2.5004 (0.013) | -1.6149 (0.108) | 0.5352 |
| | | DTI | -17.0893 (<0.001) | -2.5467 (0.012) | -3.3998 (<0.001)* | 0.5510 |
| | | Combined | -17.0071 (<0.001) | -2.5604 (0.011) | -3.0056 (0.003) | 0.5467 |
| TVA - Short-term memory storage ($K$) | 0.2013 | T1 | -7.7691 (<0.001) | -1.5196 (0.130) | -1.1179 (0.265) | 0.1981 |
| | | DTI | -7.8117 (<0.001) | -1.5383 (0.125) | -2.0302 (0.043) | 0.2070 |
| | | Combined | -7.7525 (<0.001) | -1.5195 (0.130) | -0.9537 (0.341) | 0.1970 |
| TVA - Perceptual threshold ($t_0$) | 0.0764 | T1 | 5.7303 (<0.001) | -1.9470 (0.053) | 0.9617 (0.337) | 0.1141 |
| | | DTI | 5.7333 (<0.001) | -1.9444 (0.053) | 1.1066 (0.270) | 0.1152 |
| | | Combined | 5.7523 (<0.001) | -1.9587 (0.051) | 1.8346 (0.068) | 0.1226 |
| TVA - Processing speed ($C$) | 0.1304 | T1 | -4.6692 (<0.001) | 0.3969 (0.692) | 0.8093 (0.419) | 0.0723 |
| | | DTI | -4.6800 (<0.001) | 0.4053 (0.686) | 0.1402 (0.889) | 0.0699 |
| | | Combined | -4.6827 (<0.001) | 0.3944 (0.694) | 0.8916 (0.374) | 0.0728 |
| Cluster 1 | 0.2470 | T1 | -7.1741 (<0.001) | -5.1567 (<0.001) | -0.1927 (0.847) | 0.2440 |
| | | DTI | -7.1623 (<0.001) | -5.1410 (<0.001) | 0.3683 (0.713) | 0.2443 |
| | | Combined | -7.1805 (<0.001) | -5.1641 (<0.001) | -0.3879 (0.699) | 0.2443 |
| Cluster 2 | 0.1720 | T1 | -7.2680 (<0.001) | 1.6030 (0.110) | -0.1013 (0.919) | 0.1687 |
| | | DTI | -7.2785 (<0.001) | 1.6062 (0.110) | -0.6549 (0.513) | 0.1701 |
| | | Combined | -7.2740 (<0.001) | 1.6104 (0.109) | -0.6382 (0.524) | 0.1700 |
| Cluster 3 | 0.0698 | T1 | -2.0177 (0.045) | -3.9824 (<0.001) | -0.8103 (0.419) | 0.0686 |
| | | DTI | -2.0337 (0.043) | -3.9969 (<0.001) | -1.84 (0.067) | 0.0783 |
| | | Combined | -2.0185 (0.045) | -3.9877 (<0.001) | -0.9765 (0.330) | 0.0697 |
| Cluster 4 | 0.2783 | T1 | -10.1319 (<0.001) | 1.2314 (0.219) | -2.5436 (0.012) | 0.2937 |
| | | DTI | -10.1479 (<0.001) | 1.2377 (0.217) | -2.5207 (0.012) | 0.2933 |
| | | Combined | -10.3013 (<0.001) | 1.2196 (0.224) | -3.6163 (<0.001)* | 0.3113 |

| | | | | | | |
|---|---|---|---|---|---|---|
| Cluster 5 | 0.1772 | T1 | -6.8872 (<0.001) | -2.5902 (0.010) | -1.1084 (0.269) | 0.1779 |
| | | DTI | -6.8667 (<0.001) | -2.5805 (0.010) | -0.5825 (0.561) | 0.1750 |
| | | Combined | -6.9577 (<0.001) | -2.6481 (0.009) | -1.9103 (0.057) | 0.1858 |
| Cluster 6 | 0.5092 | T1 | -15.9345 (<0.001) | -1.1148 (0.266) | -1.8971 (0.059) | 0.5145 |
| | | DTI | -15.9719 (<0.001) | -1.1080 (0.269) | -2.0875 (0.038) | 0.5160 |
| | | Combined | -16.0156 (<0.001) | -1.1196 (0.264) | -2.459 (0.015) | 0.5193 |
| Cluster 7 | 0.1399 | T1 | -6.4852 (<0.001) | -0.7736 (0.440) | -0.3433 (0.732) | 0.1369 |
| | | DTI | -6.5210 (<0.001) | -0.7689 (0.443) | -1.6007 (0.111) | 0.1452 |
| | | Combined | -6.4926 (<0.001) | -0.7759 (0.439) | -0.63 (0.529) | 0.1379 |

Table 2. Cognitive associations with BAG – statistics. * FDR significant ** Bonferroni significant.

870 **Supplementary Figures**

871
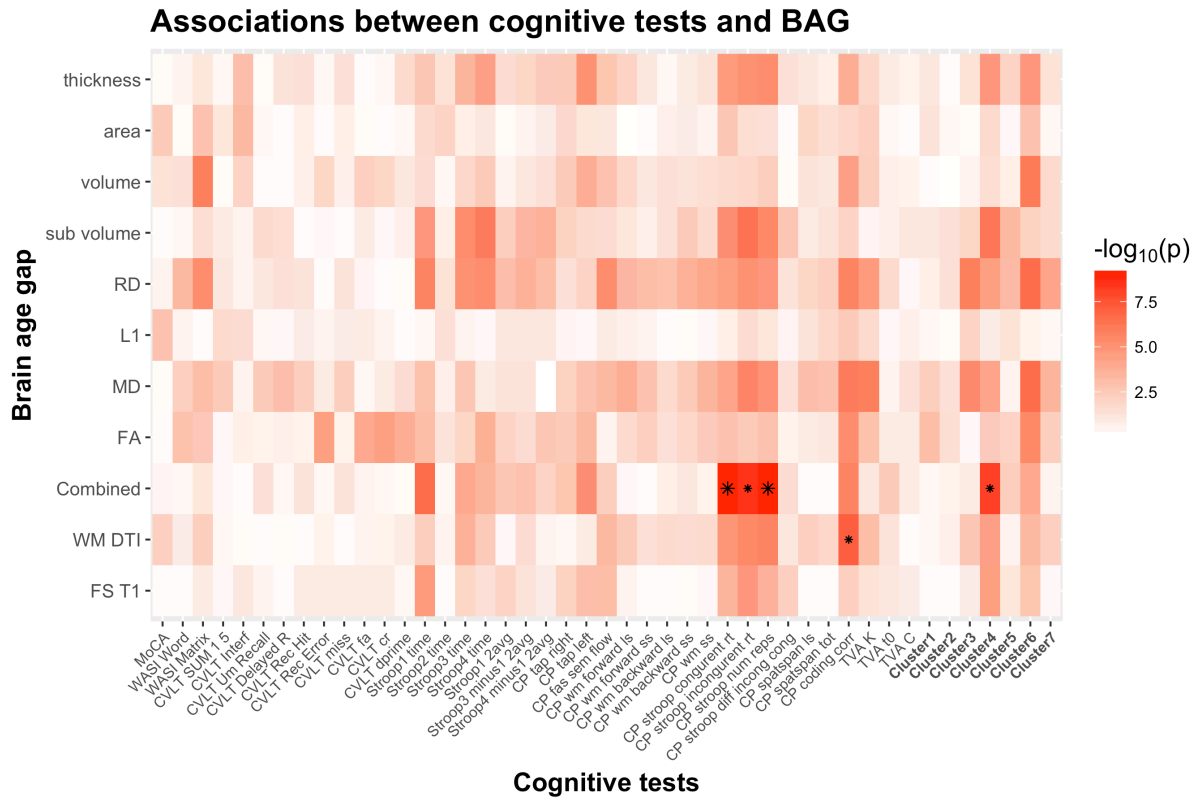


872

873 **Fig. S1.** Heatmap of the association between cognitive scores and brain age gaps using non-

874 linear models, including age, age$^2$ and sex as covariates. The color scale depicts the minus log

875 of the p-values (-log$_{10}$(p)) for each association. The association marked with a small star

876 represents significant associations after FDR correction, and the one marked with a big star

877 shows significant associations after Bonferroni correction.

878

879

880

881

882

883

884

885

886

887

888

889 **Supplementary Tables**

890 Cognitive associations with Brain Age Gap (BAG) using non-linear models, including age,

891 age$^2$ and sex as covariates – statistics.

| Test | Adj R$^2$ no-BAG | BAG | Main effect Age t(p) | Main effect Age$^2$ t(p) | Main effect Sex t(p) | Main effect BAG t(p) | Adj R$^2$ |
|---|---|---|---|---|---|---|---|
| MoCA | 0.088 | T1 | -4.5563 (<0.001) | -0.2752 (0.7834) | -2.1792 (0.0302) | -0.1146 (0.9088) | 0.0845 |
| | | DTI | -4.5575 (<0.001) | -0.3078 (0.7585) | -2.1727 (0.0307) | 1.5937 (0.1122) | 0.0934 |
| | | Combined | -4.561 (<0.001) | -0.2413 (0.8095) | -2.1894 (0.0295) | -0.4399 (0.6604) | 0.0851 |
| WASI words | 0.0792 | T1 | 4.7079 (<0.001) | -1.5614 (0.1197) | 0.4698 (0.6389) | -0.1719 (0.8637) | 0.0756 |
| | | DTI | 4.7017 (<0.001) | -1.5532 (0.1216) | 0.4775 (0.6334) | -0.7843 (0.4336) | 0.0778 |
| | | Combined | 4.7058 (<0.001) | -1.5325 (0.1266) | 0.4655 (0.642) | -0.3554 (0.7226) | 0.076 |
| WASI matrix | 0.1825 | T1 | -7.6085 (<0.001) | -1.3223 (0.1873) | 0.048 (0.9618) | -0.8787 (0.3804) | 0.1817 |
| | | DTI | -7.6627 (<0.001) | -1.311 (0.1911) | 0.0606 (0.9517) | -1.6227 (0.1059) | 0.1876 |
| | | Combined | -7.6132 (<0.001) | -1.2678 (0.206) | 0.0407 (0.9676) | -1.0117 (0.3126) | 0.1825 |
| CVLT learning 1-5 | 0.1757 | T1 | -5.0181 (<0.001) | 0.5198 (0.6036) | -5.2162 (<0.001) | -0.2662 (0.7903) | 0.1727 |
| | | DTI | -5.0228 (<0.001) | 0.5204 (0.6032) | -5.2181 (<0.001) | -0.3723 (0.71) | 0.1729 |
| | | Combined | -5.0196 (<0.001) | 0.5363 (0.5922) | -5.2205 (<0.001) | -0.2959 (0.7675) | 0.1727 |
| CVLT interference | 0.0593 | T1 | -4.3175 (<0.001) | -0.062 (0.9506) | -0.3788 (0.7051) | -0.9545 (0.3407) | 0.0589 |
| | | DTI | -4.3143 (<0.001) | -0.086 (0.9316) | -0.3772 (0.7064) | -0.2366 (0.8132) | 0.0558 |
| | | Combined | -4.3124 (<0.001) | -0.075 (0.9403) | -0.3794 (0.7047) | -0.1796 (0.8576) | 0.0557 |
| CVLT recall | 0.2401 | T1 | -6.4676 (<0.001) | 0.6091 (0.543) | -5.8925 (<0.001) | -0.5048 (0.6141) | 0.2379 |
| | | DTI | -6.4667 (<0.001) | 0.5965 (0.5514) | -5.8892 (<0.001) | -0.1381 (0.8902) | 0.2371 |
| | | Combined | -6.4859 (<0.001) | 0.6973 (0.4863) | -5.9255 (<0.001) | -1.1682 (0.2438) | 0.2412 |
| CVLT delayed recall | 0.1822 | T1 | -4.9433 (<0.001) | 0.6624 (0.5083) | -5.4919 (<0.001) | 0.1193 (0.9052) | 0.179 |
| | | DTI | -4.9411 (<0.001) | 0.6618 (0.5087) | -5.4912 (<0.001) | 0.2079 (0.8354) | 0.1791 |
| | | Combined | -4.9454 (<0.001) | 0.6981 (0.4857) | -5.4986 (<0.001) | -0.3668 (0.7141) | 0.1794 |
| CVLT recognition hits | 0.0464 | T1 | -2.615 (0.0095) | -0.3694 (0.7121) | -2.5144 (0.0125) | -0.8444 (0.3992) | 0.0453 |
| | | DTI | -2.6175 (0.0094) | -0.3994 (0.6899) | -2.504 (0.0129) | 0.1039 (0.9173) | 0.0427 |
| | | Combined | -2.622 (0.0093) | -0.3004 (0.7641) | -2.5328 (0.0119) | -1.0382 (0.3002) | 0.0467 |
| CVLT recognition errors | 0.1567 | T1 | 5.2609 (<0.001) | 1.4118 (0.1592) | 3.7395 (<0.001) | -0.8964 (0.3709) | 0.1561 |
| | | DTI | 5.2485 (<0.001) | 1.3947 (0.1643) | 3.7336 (<0.001) | -0.5993 (0.5495) | 0.1546 |
| | | Combined | 5.2514 (<0.001) | 1.4099 (0.1598) | 3.7277 (<0.001) | -0.3837 (0.7015) | 0.1539 |
| CVLT recog misses | 0.0464 | T1 | 2.615 (0.0095) | 0.3694 (0.7121) | 2.5144 (0.0125) | 0.8444 (0.3992) | 0.0453 |
| | | DTI | 2.6175 (0.0094) | 0.3994 (0.6899) | 2.504 (0.0129) | -0.1039 (0.9173) | 0.0427 |
| | | Combined | 2.622 (0.0093) | 0.3004 (0.7641) | 2.5328 (0.0119) | 1.0382 (0.3002) | 0.0467 |
| CVLT recog false alarm | 0.1191 | T1 | 4.4883 (<0.001) | 1.4053 (0.1612) | 3.1557 (0.0018) | -0.8236 (0.411) | 0.1179 |
| | | DTI | 4.4728 (<0.001) | 1.3906 (0.1656) | 3.1567 (0.0018) | -0.5544 (0.5798) | 0.1167 |
| | | Combined | 4.4784 (<0.001) | 1.4159 (0.158) | 3.1475 (0.0018) | -0.4786 (0.6326) | 0.1164 |
| CVLT recog correct rejection | 0.1567 | T1 | -5.2609 (<0.001) | -1.4118 (0.1592) | -3.7395 (<0.001) | 0.8964 (0.3709) | 0.1561 |
| | | DTI | -5.2485 (<0.001) | -1.3947 (0.1643) | -3.7336 (<0.001) | 0.5993 (0.5495) | 0.1546 |
| | | Combined | -5.2514 (<0.001) | -1.4099 (0.1598) | -3.7277 (<0.001) | 0.3837 (0.7015) | 0.1539 |
| CVLT d' | 0.1548 | T1 | -5.0157 (<0.001) | -0.7018 (0.4835) | -4.1938 (<0.001) | 0.3855 (0.7002) | 0.1519 |

| | | | | | | | |
|---|---|---|---|---|---|---|---|
| | | DTI | -5.0104 (<0.001) | -0.7106 (0.478) | -4.1973 (<0.001) | 0.8695 (0.3854) | 0.1539 |
| | | Combined | -5.0122 (<0.001) | -0.7079 (0.4796) | -4.1897 (<0.001) | 0.2343 (0.8149) | 0.1516 |
| STROOP 1 | 0.1181 | T1 | 5.2178 (<0.001) | 1.8817 (0.061) | 1.9786 (0.0489) | 2.6477 (0.0086) | 0.1385 |
| | | DTI | 5.1698 (<0.001) | 1.915 (0.0566) | 1.9488 (0.0524) | 1.6361 (0.103) | 0.1239 |
| | | Combined | 5.2707 (<0.001) | 1.7146 (0.0876) | 2.0444 (0.0419) | 3.243 (0.0013) | 0.1499 |
| STROOP 2 | 0.0565 | T1 | 2.955 (0.0034) | 1.8769 (0.0617) | 1.7273 (0.0853) | 0.0898 (0.9286) | 0.0528 |
| | | DTI | 2.9455 (0.0035) | 1.897 (0.059) | 1.7093 (0.0886) | -0.5228 (0.6016) | 0.0538 |
| | | Combined | 2.9595 (0.0034) | 1.8439 (0.0664) | 1.7389 (0.0833) | 0.3307 (0.7411) | 0.0531 |
| STROOP 3 | 0.2519 | T1 | 7.9387 (<0.001) | 4.0215 (<0.001)** | 2.0391 (0.0425) | 1.4584 (0.146) | 0.2552 |
| | | DTI | 8.0033 (<0.001) | 4.0506 (<0.001)** | 2.0666 (0.0398) | 2.245 (0.0256) | 0.2635 |
| | | Combined | 8.0064 (<0.001) | 3.9001 (<0.001)** | 2.0915 (0.0375) | 2.3542 (0.0193) | 0.265 |
| STROOP 4 | 0.2092 | T1 | 7.727 (<0.001) | 2.7144 (0.0071) | 1.1078 (0.269) | 1.1959 (0.2329) | 0.2105 |
| | | DTI | 7.7745 (<0.001) | 2.7322 (0.0067) | 1.1277 (0.2605) | 1.7316 (0.0846) | 0.2154 |
| | | Combined | 7.8094 (<0.001) | 2.5945 (0.01) | 1.1659 (0.2448) | 2.2006 (0.0287) | 0.221 |
| STROOP mean 1 and 2 | 0.1065 | T1 | 4.6014 (<0.001) | 2.1809 (0.0301) | 1.8851 (0.0606) | 1.5137 (0.1314) | 0.1111 |
| | | DTI | 4.5693 (<0.001) | 2.2194 (0.0274) | 1.8487 (0.0657) | 0.3205 (0.7489) | 0.1033 |
| | | Combined | 4.6255 (<0.001) | 2.0629 (0.0402) | 1.9411 (0.0534) | 1.8349 (0.0677) | 0.1148 |
| STROOP 3 minus mean 1 and 2 | 0.2486 | T1 | 7.6928 (<0.001) | 4.0734 (<0.001)** | 2.0223 (0.0442) | 1.0347 (0.3018) | 0.2488 |
| | | DTI | 7.7161 (<0.001) | 4.0759 (<0.001)** | 2.0485 (0.0416) | 1.2741 (0.2038) | 0.2504 |
| | | Combined | 7.7517 (<0.001) | 3.9419 (<0.001)** | 2.0994 (0.0368) | 1.8804 (0.0612) | 0.2561 |
| STROOP 4 minus mean 1 and 2 | 0.2225 | T1 | 7.7912 (<0.001) | 3.224 (0.0014)* | 1.0274 (0.3052) | 0.7875 (0.4317) | 0.2213 |
| | | DTI | 7.7853 (<0.001) | 3.233 (0.0014)* | 1.0273 (0.3053) | 0.5573 (0.5778) | 0.2203 |
| | | Combined | 7.8437 (<0.001) | 3.1135 (0.0021)* | 1.0945 (0.2748) | 1.4951 (0.1362) | 0.2263 |
| CP - Right motor speed | 0.3621 | T1 | -12.2583 (<0.001) | 0.4241 (0.6718) | -0.4499 (0.6532) | -1.56 (0.12) | 0.3656 |
| | | DTI | -12.201 (<0.001) | 0.3813 (0.7033) | -0.4415 (0.6592) | -0.3491 (0.7273) | 0.3599 |
| | | Combined | -12.2818 (<0.001) | 0.5259 (0.5994) | -0.4741 (0.6358) | -1.8479 (0.0658) | 0.368 |
| CP - Left motor speed | 0.3586 | T1 | -12.1901 (<0.001) | -1.3758 (0.1701) | 0.5329 (0.5946) | -1.9551 (0.0517) | 0.3656 |
| | | DTI | -12.1163 (<0.001) | -1.4124 (0.159) | 0.5396 (0.5899) | -0.8474 (0.3976) | 0.3579 |
| | | Combined | -12.2849 (<0.001) | -1.2158 (0.2252) | 0.4997 (0.6177) | -2.7995 (0.0055) | 0.3752 |
| CP - FAS semantic flow | 0.1047 | T1 | -3.0413 (0.0026) | -2.5748 (0.0106) | -3.2544 (0.0013) | -2.0265 (0.0437) | 0.1153 |
| | | DTI | -3.0473 (0.0025) | -2.6035 (0.0098) | -3.2424 (0.0013) | -2.0796 (0.0385) | 0.116 |
| | | Combined | -3.0316 (0.0027) | -2.4889 (0.0134) | -3.2639 (0.0012) | -1.642 (0.1018) | 0.1105 |
| CP - Visual WM forward ls | 0.0897 | T1 | -5.3048 (<0.001) | -0.2803 (0.7795) | 0.3424 (0.7323) | -0.5645 (0.5729) | 0.0873 |
| | | DTI | -5.3364 (<0.001) | -0.2747 (0.7838) | 0.352 (0.7252) | -1.71 (0.0885) | 0.0966 |
| | | Combined | -5.3039 (<0.001) | -0.2873 (0.7742) | 0.3445 (0.7307) | -0.2836 (0.7769) | 0.0864 |
| CP - Visual WM forward ss | 0.1388 | T1 | -6.5947 (<0.001) | -0.6439 (0.5202) | -0.0916 (0.9271) | -0.1756 (0.8608) | 0.1355 |
| | | DTI | -6.6142 (<0.001) | -0.6289 (0.53) | -0.0903 (0.9281) | -1.1522 (0.2503) | 0.1399 |
| | | Combined | -6.5945 (<0.001) | -0.657 (0.5118) | -0.0873 (0.9305) | 0.0421 (0.9664) | 0.1354 |
| CP - Visual WM backward ls | 0.0852 | T1 | -4.6076 (<0.001) | -0.9343 (0.351) | -1.567 (0.1184) | -0.068 (0.9458) | 0.0816 |
| | | DTI | -4.6299 (<0.001) | -0.9132 (0.362) | -1.5757 (0.1163) | -1.3135 (0.1902) | 0.0878 |
| | | Combined | -4.6163 (<0.001) | -0.8736 (0.3831) | -1.5842 (0.1144) | -0.7237 (0.4699) | 0.0835 |
| CP - Visual WM backward ss | 0.1026 | T1 | -5.4768 (<0.001) | -0.619 (0.5365) | -0.8352 (0.4044) | -0.2473 (0.8049) | 0.0993 |

| | | | | | | | |
|---|---|---|---|---|---|---|---|
| | | DTI | -5.4994 (<0.001) | -0.604 (0.5464) | -0.8389 (0.4023) | -1.2897 (0.1983) | 0.105 |
| | | Combined | -5.4903 (<0.001) | -0.5466 (0.5852) | -0.8555 (0.3931) | -0.9558 (0.3401) | 0.1023 |
| CP - Visual WM ss | 0.1618 | T1 | -7.0453 (<0.001) | -0.9494 (0.3433) | -0.6911 (0.4902) | -0.2639 (0.7921) | 0.1588 |
| | | DTI | -7.0749 (<0.001) | -0.9354 (0.3504) | -0.6944 (0.4881) | -1.3432 (0.1804) | 0.1645 |
| | | Combined | -7.051 (<0.001) | -0.9076 (0.365) | -0.7016 (0.4836) | -0.5866 (0.558) | 0.1597 |
| CP - Spatial stroop congruent | 0.2152 | T1 | 8.6103 (<0.001) | 0.5061 (0.6132) | -1.099 (0.2728) | 2.1677 (0.0311) | 0.2265 |
| | | DTI | 8.6646 (<0.001) | 0.539 (0.5904) | -1.1012 (0.2719) | 2.6844 (0.0078) | 0.234 |
| | | Combined | 8.8148 (<0.001) | 0.27 (0.7874) | -1.0172 (0.3101) | 3.8562 (<0.001)** | 0.2561 |
| CP - Spatial stroop incongruent | 0.2498 | T1 | 9.5215 (<0.001) | -0.3129 (0.7546) | -0.6399 (0.5228) | 2.6625 (0.0083) | 0.2674 |
| | | DTI | 9.5663 (<0.001) | -0.2497 (0.803) | -0.6711 (0.5028) | 2.8797 (0.0043) | 0.2708 |
| | | Combined | 9.6908 (<0.001) | -0.5285 (0.5976) | -0.5807 (0.5619) | 3.8325 (<0.001)* | 0.2883 |
| CP - Spatial stroop numb of reps | 0.2613 | T1 | -9.7578 (<0.001) | -0.1542 (0.8776) | 1.2196 (0.2237) | -2.2091 (0.0281) | 0.2725 |
| | | DTI | -9.8334 (<0.001) | -0.1782 (0.8587) | 1.2369 (0.2173) | -2.951 (0.0035) | 0.2831 |
| | | Combined | -9.967 (<0.001) | 0.0905 (0.928) | 1.1582 (0.2479) | -3.8672 (<0.001)** | 0.2999 |
| CP - Spatial stroop incong - cong | 0.1076 | T1 | 5.7387 (<0.001) | -0.9619 (0.337) | -0.4011 (0.6887) | 1.5968 (0.1116) | 0.1131 |
| | | DTI | 5.7189 (<0.001) | -0.9105 (0.3635) | -0.4223 (0.6732) | 0.9815 (0.3273) | 0.1075 |
| | | Combined | 5.7304 (<0.001) | -1.0014 (0.3176) | -0.3888 (0.6978) | 1.2835 (0.2005) | 0.1099 |
| CP - Spatspan ls | 0.3027 | T1 | -9.0803 (<0.001) | 0.8225 (0.4116) | -4.9183 (<0.001) | -0.0628 (0.95) | 0.3 |
| | | DTI | -9.1511 (<0.001) | 0.8555 (0.3931) | -4.9703 (<0.001) | -1.5904 (0.113) | 0.307 |
| | | Combined | -9.0818 (<0.001) | 0.8301 (0.4073) | -4.9202 (<0.001) | -0.1448 (0.885) | 0.3 |
| CP - Spatspan total | 0.3033 | T1 | -9.2413 (<0.001) | 0.5919 (0.5545) | -4.6451 (<0.001) | 0.085 (0.9324) | 0.3006 |
| | | DTI | -9.3007 (<0.001) | 0.6245 (0.5329) | -4.6899 (<0.001) | -1.3875 (0.1665) | 0.3059 |
| | | Combined | -9.2443 (<0.001) | 0.6028 (0.5472) | -4.6491 (<0.001) | -0.1118 (0.9111) | 0.3006 |
| CP - Coding corr | 0.5307 | T1 | -16.7381 (<0.001) | -0.3279 (0.7433) | -2.3396 (0.0201) | -1.596 (0.1117) | 0.5335 |
| | | DTI | -17.0629 (<0.001) | -0.3481 (0.7281) | -2.3804 (0.018) | -3.3875 (<0.001)* | 0.5495 |
| | | Combined | -16.9736 (<0.001) | -0.1442 (0.8855) | -2.4411 (0.0153) | -2.976 (0.0032) | 0.5449 |
| TVA - Short-term memory storage ($K$) | 0.1941 | T1 | -7.7533 (<0.001) | -0.0891 (0.9291) | -1.4529 (0.1475) | -1.1129 (0.2668) | 0.1949 |
| | | DTI | -7.7958 (<0.001) | -0.0894 (0.9288) | -1.471 (0.1426) | -2.0247 (0.044) | 0.2039 |
| | | Combined | -7.7352 (<0.001) | -0.0343 (0.9726) | -1.4655 (0.144) | -0.9449 (0.3456) | 0.1938 |
| TVA - Perceptual threshold ($t_0$) | 0.1146 | T1 | 5.7716 (<0.001) | 0.9866 (0.3248) | -2.1312 (0.034) | 0.9264 (0.3551) | 0.1141 |
| | | DTI | 5.7764 (<0.001) | 1.0081 (0.3144) | -2.1342 (0.0338) | 1.0951 (0.2745) | 0.1153 |
| | | Combined | 5.784 (<0.001) | 0.8478 (0.3973) | -2.1074 (0.0361) | 1.7412 (0.0829) | 0.1217 |
| TVA - Processing speed ($C$) | 0.0699 | T1 | -4.66 (<0.001) | 0.1122 (0.9107) | 0.3556 (0.7225) | 0.804 (0.4222) | 0.0686 |
| | | DTI | -4.6708 (<0.001) | 0.135 (0.8927) | 0.3579 (0.7207) | 0.1387 (0.8898) | 0.0662 |
| | | Combined | -4.6734 (<0.001) | 0.0619 (0.9507) | 0.3657 (0.7149) | 0.8815 (0.3789) | 0.0691 |
| Cluster 1 | 0.2446 | T1 | -7.1703 (<0.001) | -0.4829 (0.6296) | -4.8899 (<0.001) | -0.1702 (0.865) | 0.2416 |
| | | DTI | -7.1589 (<0.001) | -0.5024 (0.6158) | -4.8709 (<0.001) | 0.3825 (0.7024) | 0.242 |
| | | Combined | -7.1752 (<0.001) | -0.4542 (0.6501) | -4.8989 (<0.001) | -0.3391 (0.7349) | 0.2419 |
| Cluster 2 | 0.1695 | T1 | -7.2665 (<0.001) | -0.5147 (0.6072) | 1.6797 (0.0943) | -0.0814 (0.9352) | 0.1662 |
| | | DTI | -7.2772 (<0.001) | -0.5154 (0.6068) | 1.6829 (0.0937) | -0.6514 (0.5154) | 0.1676 |
| | | Combined | -7.2707 (<0.001) | -0.4611 (0.6451) | 1.6725 (0.0957) | -0.5914 (0.5548) | 0.1674 |
| Cluster 3 | 0.0767 | T1 | -2.065 (0.0399) | -1.6934 (0.0916) | -3.4589 (<0.001) | -0.7735 (0.4399) | 0.0753 |

|  |  |  |  |  |  |  |  |
|---|---|---|---|---|---|---|---|
|  |  | DTI | -2.0812 (0.0384) | -1.693 (0.0917) | -3.4728 (<0.001) | -1.8207 (0.0698) | 0.0849 |
|  |  | Combined | -2.0636 (0.0401) | -1.6405 (0.1021) | -3.4746 (<0.001) | -0.848 (0.3972) | 0.0757 |
| Cluster 4 | 0.2757 | T1 | -10.1014 (<0.001) | 0.3766 (0.7068) | 1.098 (0.2733) | -2.5518 (0.0113) | 0.2912 |
|  |  | DTI | -10.118 (<0.001) | 0.31 (0.7568) | 1.1208 (0.2635) | -2.5199 (0.0124) | 0.2908 |
|  |  | Combined | -10.2703 (<0.001) | 0.5794 (0.5629) | 1.0357 (0.3014) | -3.6468 (<0.001)* | 0.3095 |
| Cluster 5 | 0.2124 | T1 | -7.1604 (<0.001) | -3.4563 (<0.001)* | -1.6891 (0.0924) | -1.0197 (0.3089) | 0.2125 |
|  |  | DTI | -7.1405 (<0.001) | -3.4709 (<0.001)* | -1.6759 (0.095) | -0.5011 (0.6167) | 0.21 |
|  |  | Combined | -7.2104 (<0.001) | -3.3405 (0.001)* | -1.7586 (0.0799) | -1.6393 (0.1024) | 0.2177 |
| Cluster 6 | 0.51 | T1 | -15.9382 (<0.001) | -1.0984 (0.2732) | -0.8171 (0.4147) | -1.8518 (0.0653) | 0.5149 |
|  |  | DTI | -15.9778 (<0.001) | -1.1226 (0.2627) | -0.8054 (0.4214) | -2.0589 (0.0406) | 0.5165 |
|  |  | Combined | -16.0092 (<0.001) | -0.9591 (0.3385) | -0.8532 (0.3944) | -2.3608 (0.019) | 0.5191 |
| Cluster 7 | 0.1381 | T1 | -6.5016 (<0.001) | -0.6594 (0.5102) | -0.5961 (0.5516) | -0.3018 (0.7631) | 0.135 |
|  |  | DTI | -6.5363 (<0.001) | -0.643 (0.5208) | -0.5958 (0.5518) | -1.5824 (0.1148) | 0.1432 |
|  |  | Combined | -6.5065 (<0.001) | -0.6229 (0.5339) | -0.6062 (0.5449) | -0.5676 (0.5708) | 0.1358 |

892 **Table S1.** Cognitive associations with Brain Age Gap (BAG) using non-linear models,

893 including age, $age^2$ and sex as covariates – statistics. * FDR significant ** Bonferroni

894 significant.

895